

AF A163 751

DETERMINATION OF INITIAL CHEMICAL STEPS IN  
THE GAS-PHASE DECOMPOSITION OF ENERGETIC MOLECULES

FINAL TECHNICAL REPORT

DONALD F. MCMILLEN AND DAVID M. GOLDEN

DECEMBER 12, 1985

U.S. ARMY RESEARCH OFFICE

CONTRACT NO. DAAG29-82-K-0169

SRI International  
Department of Chemical Kinetics  
Chemical Physics Laboratory  
Menlo Park, CA 94025

APPROVED FOR PUBLIC RELEASE:  
DISTRIBUTION UNLIMITED.

DTIC  
ELECTE  
FEB 10 1986  
S D

DTIC FILE COPY

86 2 7 120

REPORT DOCUMENTATION PAGE		READ INSTRUCTIONS BEFORE COMPLETING FORM
1. REPORT NUMBER FINAL TECHNICAL <b>AR 19328.1-CH</b>	2. GOVT ACCESSION NO.	3. RECIPIENT'S CATALOG NUMBER
4. TITLE (and Subtitle) DETERMINATION OF INITIAL CHEMICAL STEPS IN THE GAS-PHASE DECOMPOSITION OF ENERGETIC MOLECULES		5. TYPE OF REPORT & PERIOD COVERED Final Technical Report September 1982 thru Aug'85
7. AUTHOR(s) Donald F. McMillen and David M. Golden		6. PERFORMING ORG. REPORT NUMBER PYU-4814
9. PERFORMING ORGANIZATION NAME AND ADDRESS Department of Chemical Kinetics SRI International Menlo Park, CA 94025		8. CONTRACT OR GRANT NUMBER(s) DAAG29-82-K-0169
11. CONTROLLING OFFICE NAME AND ADDRESS U. S. Army Research Office Post Office Box 12211 Research Triangle Park, NC 27709		10. PROGRAM ELEMENT, PROJECT, TASK AREA & WORK UNIT NUMBERS Physical Sciences Chemical Physics Laboratory
14. MONITORING AGENCY NAME & ADDRESS (if different from Controlling Office)		12. REPORT DATE 9 January 1986
		13. NUMBER OF PAGES 27 plus appendices
		15. SECURITY CLASS. (of this report) Unclassified
		15a. DECLASSIFICATION/DOWNGRADING SCHEDULE
16. DISTRIBUTION STATEMENT (of this Report)  Approved for public release; distribution unlimited.		
17. DISTRIBUTION STATEMENT (of the abstract entered in Block 20, if different from Report)		
18. SUPPLEMENTARY NOTES THE VIEW, OPINIONS, AND/OR FINDINGS CONTAINED IN THIS REPORT ARE THOSE OF THE AUTHOR(S) AND SHOULD NOT BE CONSTRUED AS AN OFFICIAL DEPARTMENT OF THE ARMY POSITION, POLICY, OR DE- CISION, UNLESS SO DESIGNATED BY OTHER DOCUMENTATION.		
19. KEY WORDS (Continue on reverse side if necessary and identify by block number)  nitroaromatics, TNT, gas-phase thermal decomposition, kinetics, mechanism, laser pyrolysis		
20. ABSTRACT (Continue on reverse side if necessary and identify by block number)  Laser-powered homogeneous pyrolysis (LPHP) has been successfully used to provide conditions where surface-sensitive substrates can be indirectly heated by an infrared laser and allowed to react while remote from potentially catalytic surfaces. The use of the comparative rate technique with LPHP provides an accur- ate indirect temperature measurement and has made practical the extraction of thermal decomposition Arrhenius parameters. A laser-heated, GC/MS-monitored, stirred-flow reaction cell has been used with cyclohexene as the internal		

temperature standard to determine Arrhenius parameters for the homogeneous gas phase thermal decomposition of nitrobenzene (NB), meta-dinitrobenzene (m-DNB), para-nitrotoluene (p-NT), ortho-nitrotoluene (o-NT), and 2,4-dinitrotoluene (2,4-DNT). In all cases the principal rate-limiting step is the homolysis of the Ar-NO<sub>2</sub> bond. The measured Arrhenius parameters for homolysis range from log A = 14.5 to 16.4, and from E<sub>a</sub> = 67.0 to 70.0 kcal/mol. The bond dissociation energies derived from the results are 71.4, 73.2, 71.4, 70.2, and 70.6 kcal/mol, respectively, for the above series of compounds.

Compound	log k (sec <sup>-1</sup> )	BDE(kcal/mol)
nitrobenzene	13.5 ± 0.5 - 68.2/ ± 1.7/2.3 RT	71.4 ± 2.0
m-dinitrobenzene	14.5 ± 0.5 - 70.0/ ± 2.1/2.3 RT	73.2 ± 2.4
p-nitrotoluene	14.9 ± 0.5 - 68.2/ ± 2.0/2.3 RT	71.4 ± 2.3
o-nitrotoluene	16.4 ± 0.6 - 67.0/ ± 2.2/2.3 RT	70.2 ± 2.5
dinitrotoluene	15.3 ± 0.4 - 67.4/ ± 1.7/2.3 RT	70.6 ± 2.0

For o-NT alone in this series, data suggest the existence of a minor decomposition pathway whose products have not yet been determined. This could reflect the onset of the as-yet unelucidated reaction mechanisms that dominate the condensed-phase reactions of ortho-substituted nitroaromatics.

The LPHP technique was also used to assess the role of C-H bond scission in the very high temperature decomposition of ethylbenzene. Contrary to a recent suggestion, initial C-C bond scission was found to be completely dominant, even at temperatures as high as 1500 K.

Preliminary results for trinitrobenzene and trinitrotoluene indicate that decomposition takes place by other pathways than initial phenyl-NO<sub>2</sub> bond scission, and that the net result is destruction of at least 50% of the aromatic rings. The recently completed molecular-beam mass spectrometrically monitored LPHP system will help to settle this issue by providing for direct, real-time observation of the initial reaction products for these and other very low-vapor pressure energetic materials. This will provide an important complement to the GC/MS monitored LPHP system, which will continue to be useful because of its ability to quantitate complex product mixtures with a very wide dynamic detection range.



January 9, 1986

Final Technical Report  
SRI Project No. 4814  
Contract No. DAAG29-82-K-0169  
Covering the Period: September 1982 through August 1985


**DETERMINATION OF INITIAL CHEMICAL STEPS IN  
THE GAS-PHASE DECOMPOSITION OF ENERGETIC MOLECULES**

By: Donald F. McMillen and David M. Golden  
Department of Chemical Kinetics  
Chemical Physics Laboratory

Prepared for:

U.S. ARMY RESEARCH OFFICE  
Box 12211  
Research Triangle Park, NC 27709  
Attention: Dr. Robert G. Ghirardelli, Director  
Chemical and Biological Sciences Division

Approved:


  
Donald C. Lorents, Laboratory Director  
Chemical Physics Laboratory

G. R. Abrahamson  
Vice President  
Physical Sciences Division



Accession For	
NTIS CRA&I	<input checked="" type="checkbox"/>
DTIC TAB	<input type="checkbox"/>
Unannounced	<input type="checkbox"/>
Justification	
By	
Distribution /	
Availability Codes	
Dist	Avail and/or Special
A-1	

# ABSTRACT


 Laser-powered homogeneous pyrolysis (LPHP) has been successfully used to provide conditions where surface-sensitive substrates can be indirectly heated by an infrared laser and allowed to react while remote from potentially catalytic surfaces. The use of the comparative rate technique with LPHP provides an accurate indirect temperature measurement and has made practical the extraction of thermal decomposition Arrhenius parameters. A laser-heated, GC/MS-monitored, stirred-flow reaction cell has been used with cyclohexene as the internal temperature standard to determine Arrhenius parameters for the homogeneous gas phase thermal decomposition of nitrobenzene (NB), meta-dinitrobenzene (m-DNB), para-nitrotoluene (p-NT), ortho-nitrotoluene (o-NT), and 2,4-dinitrotoluene (2,4-DNT). In all cases the principal rate-limiting step is the homolysis of the Ar-NO<sub>2</sub> bond. The measured Arrhenius parameters for homolysis range from log A = 14.5 to 16.4, and from E<sub>a</sub> = 67.0 to 70.0 kcal/mol. The bond dissociation energies derived from the results are 71.4, 73.2, 71.4, 70.2, and 70.6 kcal/mol, respectively, for the above series of compounds.

Compound	log k (sec <sup>-1</sup> )	BDE(kcal/mol)
nitrobenzene	15.5 ± 0.5 - 68.2/ ± 1.7/2.3 RT	71.4 ± 2.0
m-dinitrobenzene	14.5 ± 0.5 - 70.0/ ± 2.1/2.3 RT	73.2 ± 2.4
p-nitrotoluene	14.9 ± 0.5 - 68.2/ ± 2.0/2.3 RT	71.4 ± 2.3
o-nitrotoluene	16.4 ± 0.6 - 67.0/ ± 2.2/2.3 RT	70.2 ± 2.5
dinitrotoluene	15.3 ± 0.4 - 67.4/ ± 1.7/2.3 RT	70.6 ± 2.0

For o-NT alone in this series, data suggest the existence of a minor decomposition pathway whose products have not yet been determined. This could reflect the onset of the as-yet unelucidated reaction mechanisms that dominate the condensed-phase reactions of ortho-substituted nitroaromatics.

The LPHP technique was also used to assess the role of C-H bond scission in the very high temperature decomposition of ethylbenzene. Contrary to a recent suggestion, initial C-C bond scission was found to be completely dominant, even at temperatures as high as 1500 K.

Preliminary results for trinitrobenzene and trinitrotoluene indicate that decomposition takes place by other pathways than initial phenyl-NO<sub>2</sub> bond scission, and that the net result is destruction of at least 50% of the aromatic rings. The recently completed molecular-beam mass spectrometrically monitored LPHP system will help to settle this issue by providing for direct, real-time observation of the initial reaction products for these and other very low-vapor pressure energetic materials. This will provide an important complement to the GC/MS monitored LPHP system, which will continue to be useful because of its ability to quantitate complex product mixtures with a very wide dynamic detection range.

Accession For	
NTIS	CRA&
DTIC	TAB
Unannounced Justification	
By	
Distribution /	
Availability Codes	
Dist	Avail a d / or Special
AI	

## CONTENTS

ABSTRACT.....	11
INTRODUCTION.....	1
RESULTS .....	3
A. Mono- and Di-Nitro Compounds: Decomposition Via Simple Bond Scission.....	3
B. Trinitro Compounds: Decomposition to Yield Low Molecular Weight Products.....	12
C. Construction of a Molecular Beam Sampling- Laser Pyrolysis Apparatus (LPHP-3).....	17
1. Vacuum System.....	17
2. Flow Cell Operation and MB Generation.....	17
PARTICIPATING PERSONNEL.....	24
SUMMARY .....	25
REFERENCES.....	27

## APPENDICES

- A           MECHANISM OF DECOMPOSITION OF NITROAROMATICS:  
            LASER-POWERED HOMOGENEOUS PYROLYSIS OF  
            SUBSTITUTED NITROBENZENES  
            J. Phys. Chem., 1985, 89, 4809
- B           LASER PYROLYSIS OF ETHYLBENZENE: THE ROLE OF  
            C-H BOND HOMOLYSIS AT HIGH TEMPERATURES  
            An. Asoc. Quim. Argen., 1985, 73(2), 141-150

## INTRODUCTION

For many years, determination of the initial chemical steps in the decomposition of energetic materials has been a goal that has eluded researchers. During this project, the laser-powered pyrolysis technique has been successfully developed and used to study the kinetics and mechanisms of the homogeneous decomposition of moderately low volatility, high surface-sensitivity energetic materials. The following tasks have been accomplished:

- (1) Construction of the second generation heated-flow-cell/heated-inlet-system, GC-monitored laser-powered homogenous pyrolysis apparatus (LPHP-2)
- (2) Conversion of the GC detection system to a GC/MS system
- (3) Use of LPHP-2 to determine the products and Arrhenius parameters for the gas-phase thermal decomposition of:
  - nitrobenzene
  - ortho-nitrotoluene
  - meta-dinitrobenzene
  - para-nitrotoluene
  - 2,4-dinitrotoluene
- (4) Use of LPHP-2 to obtain preliminary rate measurements for the gas-phase thermal decomposition of trinitrobenzene and trinitrotoluene
- (5) Use of LPHP-2 to study ethylbenzene and help settle a controversy over the products and mechanism of its very high temperature decomposition
- (6) Design and construction of a molecular-beam mass spectrometrically detected laser pyrolysis system (LPHP-3) that will detect the initial products directly, without the need to trap reactive species with scavengers.

In addition, AFOSR funding (now in its first year) has allowed us to supplement these efforts by a parallel study focusing on nitramines. Thus far, this work has resulted in the use of LPHP-2 to obtain rate and product



determination and preliminary Arrhenius parameter measurements for dimethylnitramine and dimethylnitrosamine, and is currently being used to test out the newly constructed molecular-beam LPHP-3 system.

Results listed under items (3) and (5) are briefly summarized in the next section, and are fully described in published papers, reprints of which are included as Appendices A and B. The report includes some additional discussion and comparison of the nitroaromatic decomposition results with the heated single-pulse shock tube results of Tsang. The report also presents a brief description of the results for dimethylnitramine and the trinitroaromatic decomposition, as well as a description and discussion of certain design considerations for the molecular beam LPHP system.

## RESULTS

### A. Mono- and Di-Nitro Compounds: Decomposition Via Simple Bond Scission

Laser-powered-homogeneous pyrolysis (LPHP)<sup>1</sup> has been used to study the gas-phase thermal decomposition of nitrobenzene (NB), *m*-dinitrobenzene (*m*-DNB), *p*-nitrotoluene (*p*-NT), *o*-nitrotoluene (*o*-NT), and 2,4-dinitrotoluene (2,4-DNT) under conditions where surface-catalyzed reactions are precluded. These results are described in detail in Appendix A. The Arrhenius parameters have been determined by comparative rate measurements relative to cyclohexene decomposition and the dominant reaction mechanisms have been established. In all cases, the principal rate-limiting step is the homolysis of the Ar-NO<sub>2</sub> bond. The measured Arrhenius parameters and the bond dissociation energies for the C-NO<sub>2</sub> have been derived from these results.

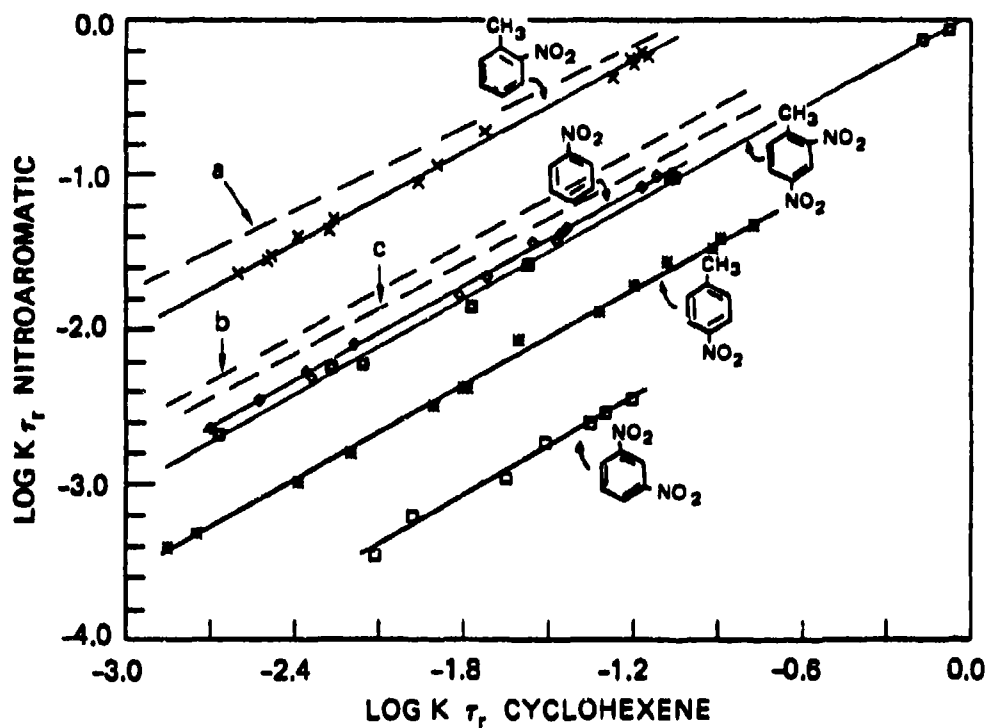
Compound	log k (sec <sup>1</sup> )	BDE(kcal/mol)
nitrobenzene	15.5 ± 0.5 - 68.2/ ± 1.7/2.3 RT	71.4 ± 2.0
<i>m</i> -dinitrobenzene	14.5 ± 0.5 - 70.0/ ± 2.1/2.3 RT	73.2 ± 2.4
<i>p</i> -nitrotoluene	14.9 ± 0.5 - 68.2/ ± 2.0/2.3 RT	71.4 ± 2.3
<i>o</i> -nitrotoluene	16.4 ± 0.6 - 67.0/ ± 2.2/2.3 RT	70.2 ± 2.5
dinitrotoluene	15.3 ± 0.4 - 67.4/ ± 1.7/2.3 RT	70.6 ± 2.0

The description of these results in Appendix A includes some comparison with the preliminary results obtained by Tsang<sup>2</sup> for the three mononitro compounds in the above list using a heated single-pulse shock-tube (SPST). There are complexities in the nitrotoluene decomposition not discussed in the short summary given above. These complexities are responsible for some of the differences between the SRI results obtained with LPHP and the results obtained by Tsang with the SPST technique. It is important to determine the extent to which these differences merely

represent experimental scatter in either or both of the methods, and the extent to which they reflect differing competition between alternative reaction pathways under somewhat different reaction conditions. To this end, we have compared the results and outlined below the various differing experimental factors in the two experimental techniques.

In trying to understand the implications of the differences between the SPST results and LPHP results, it is important to first understand the extent of the agreement. The absolute rates determined by the two techniques for nitrobenzene are in good agreement, differing only by a factor of 1.7 ( $\Delta G^\ddagger$  at 1200 K = 1.3 kcal/mol). Moreover, the measured nitrobenzene Arrhenius parameters (for  $k_{uni}$ ) are also very close. The extent of this agreement can be seen in Figure 1 and Table 1, where the LPHP and SPST results are compared for each of the three substrates that have so far been studied by both techniques. The figure offers an immediate visual impression of the extent of agreement. However, it does not show that the LPHP results are lowered by about 0.1 log unit because the bond scission reaction was slightly in the falloff under the LPHP conditions, whereas the SPST conditions (pressure 3 atm vs. 0.4 atm in LPHP) provided reaction at the high pressure limit. This factor is taken into account in Table 1. Note that the temperature "calibration" of the abscissa (the horizontal location of the dashed lines) is found by taking the value of  $\tau$  as that which makes the vertical distances to the appropriate solid lines equal to the differences in the log  $k$  values (columns 2 and 8, Table 1), corresponding to the actual measured Arrhenius parameters. The value of  $\tau$  (10  $\mu$ s) that produced the correspondence is an "average" reaction time and an "effective" reaction temperature. That this value of  $\tau$  happens to agree almost exactly with the normal reaction time that we commonly use and that was derived from the time behavior of spatially averaged infrared fluorescence measurements indicates that the actual peak temperatures are not far above the "effective" reaction temperatures, i.e., the reaction does not take place in a small fraction of the nominally heated volume at temperatures far higher than the "effective" reaction temperature.

Not only are the results for nitrobenzene in very good agreement, but also the total rates of disappearance of ortho-nitrotoluene (o-NT) are also



JA-4814-3A

FIGURE 1 LPHP COMPARATIVE RATE PLOT FOR  $\text{ArNO}_2$  DECOMPOSITION

Dashed lines a, b, c, correspond to SPST parameters from Tsang.

(a) ortho-nitrotoluene (see footnote a in Table 1).

(b) nitrobenzene

(c) para-nitrotoluene.

Table 1

COMPARISON OF LPHP- AND SPST-DERIVED  
ARRHENIUS PARAMETERS FOR  $\text{ArNO}_2$  DECOMPOSITION

Substrate	log $k_x$ , 1200		log $A_x$ , $E_x$		SRI $k_\infty$	SRI $k_x/k_\infty$	Tsang $k_x$ adj
	SRI	Tsang	SRI	Tsang			
o-nitrotoluene	3.97	3.75	15.9, 65.5	14.95, 61.5	4.09	0.75	4.15
nitrobenzene	3.09	3.32	15.2, 66.5	15.25, 65.5	3.17	0.84	
2,4-DNT	3.00	- - -	15.2, 67	- - - -	3.02	0.96	
p-nitrotoluene	2.45	3.21	14.8, 67.8	14.9, 64.2	2.47	0.96	
m-dinitrobenzene	1.75	- - -	14.5, 70.0	- - - -	1.75	(1.0)	

<sup>a</sup>"Adjustment" to log  $k = + \log$  (LPHP/SPST mass balance ratio).

in reasonable agreement, when we consider that the LPHP-derived parameters reflect a fair mass balance (75%) and the SPST-derived parameters reflect the recovery of substantially less (29% to 34% over the experimental temperature range) toluene from the decomposed o-NT. [In both techniques, the ratio of substrate at time zero to unreacted substrate at time t required for calculation of the decomposition rate constant is provided by the ratio: (products + unreacted substrate)/(unreacted substrate).] Thus, with both techniques the total rates of disappearance of o-NT are similar, but different amounts of substrate are lost to the as-yet unknown pathway. The possible reasons for the different degrees of loss are discussed below.

The most perplexing point of disagreement at this point is the reaction of para-nitrotoluene (p-NT). Whereas the LPHP results show p-NT to react at ~ 25% of the rate of NB, the SPST results show the value to be about 80% of the nitrobenzene rate (corresponding to a discrepancy in  $\Delta G^\ddagger_{1200}$  for the two substrates of 2.9 kcal/mol). This disagreement is very puzzling in light of the agreement for NB and o-NT, particularly since the mass balances for p-NT are good with both techniques. That is, with o-NT and its evident interaction between the methyl group and the ortho-methyl substituent, some differences are not surprising. With p-NT, on the other hand, one would have expected the same kind of consistency between the two techniques as was seen for NB itself.

To determine whether the p-NT rate is depressed too much in the LPHP results, or too little in the SPST results, there are two other comparisons that may be made within the set of LPHP rate constants reported here. Both these comparisons involve the decomposition of 2,4-dinitrotoluene, where there is both an ortho-methyl-substituted and a para-methyl-substituted  $\text{NO}_2$ .

The first comparison is between the difference between o-NT and p-NT (and o-NT and NB) absolute rates on the one hand and the difference between o- $\text{NO}_2$  and p- $\text{NO}_2$  loss from 2,4-DNT on the other hand. From Table 1, and the 8% yield of o-NT from 2,4-DNT, we have:

Rate of p- $\text{NO}_2$  loss from DNT:

$$\Delta \log k_{\infty,1200} (\text{o-NT} - \text{p-NT}) = 4.09 - 2.47 = 1.62$$

$$\Delta \log k_{\infty,1200} (\text{o-NT} - \text{NB}) = 4.08 - 3.17 = 0.92$$

$$\Delta \log k_{\infty} (\text{o-NO}_2 \text{ loss} - \text{p-BI}_2 \text{ loss}) = \log \left( \frac{\text{yield p-NT}}{\text{yield o-NT}} \right)$$

$$= \log \left( \frac{[100 - 8]/0.96}{8} \right) = 1.08$$

The difference between o- and p-NO<sub>2</sub> loss from 2,4-DNT is greater than the difference between o-NT and NB and less than the difference between o-NT and p-NT. Taken at face value, these differences suggest either that p-methyl substitution has a somewhat smaller rate-depressing effect on loss of NO<sub>2</sub> from a ring that is already substituted with a second nitro group, or that the nominal effect of para-methyl substitution shown by the LPHP data for p-NT is indeed somewhat (0.4 to 0.5 log units) too large.

A related comparison is between the rate of p-NO<sub>2</sub> loss from 2,4-DNT and the rate of loss of one of the NO<sub>2</sub> groups in m-DNB.

Rate of p-NO<sub>2</sub> loss from DNT:

$$\log k_{\infty,1200} (2,4\text{-DNT}) - \log \left( \frac{[100 - 8]/0.96}{8} \right) = 3.02 - 1.08 = 1.94$$

$$\log k_{\infty,1200} (\text{m-DNB, per NO}_2) = 1.75 - \log 2 = 1.45$$

Here we see that the rate of loss of the p-NO<sub>2</sub> is somewhat greater (0.5 units) than the loss rate for a single -NO<sub>2</sub> from m-DNB. That is, substitution of a p-methyl group onto m-DNB actually causes an increase in the loss rate for the p-NO<sub>2</sub> group. Thus the effect of the second NO<sub>2</sub> group would appear to be diluted by the presence of a methyl group ortho- to it. Thus these two attempts to determine whether the effect of p-methyl substitution on NB is consistent with its effect on m-DNB decomposition indicate that the two rate-retarding effects are not additive (or that the precision of rate measurement for the minor pathway in 2,4-DNT decomposition is insufficient to make the comparison reliable). In either case, the data now in hand do not provide a check on the magnitude of the rate-depressing effect of p-methyl substitution.

Note that the apparent lack of additivity discussed above for two retarding effects is in contrast to the additivity demonstrated (Appendix A) for the retarding effect of *m*-NO<sub>2</sub> substitution and the accelerating effect of *o*-methyl substitution. The question of the effect of *p*-methyl substitution on NB can be settled by performing competitive decomposition experiments with a mixture of NB and *p*-NO<sub>2</sub> (or with a mixture of *p*-NT and 2,4-DNT, since competitive measurements with 2,4-DNT and *o*-NT have already been performed).

To help determine the origin of the differences discussed above, Table 2 lists the reaction conditions provided by the LPHP-2 technique and the single-pulse shock tube as used by Tsang. The principal apparent differences relate to the different reaction times or dwell times and the greater variations of temperature with time and space in the LPHP technique. The possible effects of these differences are briefly discussed below. The errors resulting from anticipated temperature-time-space inhomogeneities are fully discussed in Reference 1, where the development of the technique is described, and in References 3, where other authors also address the application of the comparative rate method to a nonisothermal laser pyrolysis technique, and in reference 4.

The first obvious difference is that in the pulsed-laser LPHP, a total reaction time similar to the 1 ms of the SPST is obtained by many heatings (typically 30 to 50) of about 10- $\mu$ s duration each. The initial LPHP cooling rate is >100 K/10  $\mu$ s versus < 10 K/10  $\mu$ s for the SPST. In a situation where active intermediates remain hot for only 1/100 of the time that they do in the SPST, one might expect some differences in the behavior of these intermediates. However, this difference does not seem to explain the particular differences seen in the *o*-NT behavior, because a phenyl radical is not easily decomposed, and since production of *o*-methylphenyl radicals by another route in the SPST leads exclusively to formation of toluene as the final product.<sup>2</sup> Thus, the greater loss of decomposed *o*-NT in the SPST is not easily attributable to some high temperature decomposition pathway for methyl substituted phenyl radicals, but appears to reflect the fact that 70% of the reaction under those conditions never involves formation of the phenyl radicals.



Table 2  
COMPARISON OF LASER PYROLYSIS AND SHOCK-TUBE REACTION  
CONDITIONS FOR NITROAROMATIC DECOMPOSITION

Parameter	LPHP	SP Shock Tube
Reaction temperature	1100-1300 K	
Reaction time	~10 $\mu$ s (x 30 pulses)	~1000 $\mu$ s
Bath gas	CO <sub>2</sub>	Ar
P <sub>tot</sub>	300 Torr	3 Atm
Substrate partial pressure	~ 0.03 Torr	~0.1 Torr
Scavengers used	o-fluorotoluene, cyclopentane	o-fluorotoluene cyclopentane
Scavenger partial pressure	~5 Torr	~30 Torr
Initial cooling rate	> 100 K/10 $\mu$ s	< 10 K/10 $\mu$ s
Scavenging conditions	10 $\mu$ s at peak T, measured over T range 800-1200 K	~1 ms at peak T
Estimated scavenging lifetime for phenyl radicals (with o-F-toluene)	~2 x 10 <sup>-3</sup> s	~2 x 10 <sup>-4</sup> s

The second obvious difference between LPHP and SPST reaction conditions is related to the recognized temperature inhomogeneities in the LPHP technique; these suggest that a significant portion of the reaction takes place at temperatures somewhat higher than the nominal peak temperature. (Note that even if the laser intensity were constant across the entire beam, cooling by an axially symmetric expansion wave traveling inward from the periphery of the laser-heated cylinder of gas results in reaction times ranging from zero at the periphery to the transit time to the axis for molecules located on the axis. This means that definition of the "average" reaction time as that transit time will result in a nominal reaction temperature somewhat lower than the actual peak temperature. (In the current case, this difference amounts to about 50 K.) Furthermore, any Gaussian distribution or inhomogeneities in the laser beam may mean that the actual peak temperature is even further above the nominal peak temperature. As restated above, error analyses<sup>1,3</sup> show that the comparative rate technique accommodates such variations very well, as long as the temperature standard has a temperature dependence close to that of the substrate, and the fractional reaction of both substances is kept below about 25% (per pulse, in the heated zone). However, in the event that decomposition of the unknown proceeds by two competitive pathways having different temperature dependence, then functioning of the LPHP system at temperatures significantly higher (say 100 to 150 K) than the nominal peak temperature could result in correct determination of the temperature dependence, but for a somewhat different branching ratio than would be seen by a SPST operating in a lower temperature range. In discussions with Tsang, this was suggested as a possible explanation because the SPST mass balance for o-NT increases from 29% at the low end of the temperature range to 34% at the upper end.

The above explanation makes qualitative sense, but seems quantitatively unlikely for the following reasons:

- (1) The real LPHP temperature range would have to be very much higher to push the mass balance from 34% to 70%.
- (2) The temperature range covered by each of the two techniques is already more than 100 K (in the range 1050 to 1250 K).

- (3) The actual LPHP peak temperature cannot exceed about 1500 K without the production of significant amounts of F atoms from the infrared absorber (the effects of which are not seen in any of these experiments).

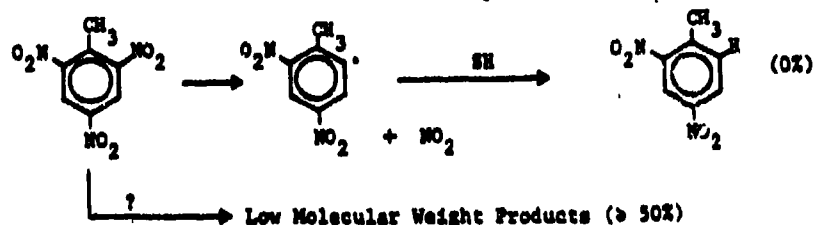
The above detailed discussion is included in this report because we assume that delineation of the factors responsible for the differing contributions of the "unspecified" process in these two systems will be an important clue to the nature of the process, and to the pathological behavior<sup>5</sup> of certain nitroaromatics that has mystified chemists for some time.

However, this discussion should not detract from the central point--namely, that the LPHP and the SPST results are in substantial agreement on several aspects of nitroaromatic decomposition. First, the total decomposition rate constants measured in the two systems are very similar for both nitrobenzene and ortho-nitrotoluene. Second, a substantial portion (70% and 30%, respectively) of the o-NT decomposition has, for the first time, been shown to take place through a "normal" phenyl-NO<sub>2</sub> scission when constrained to react in the gas phase in the absence of solid surfaces and condensed phases. Third, even under the "surface-free" conditions provided by each technique, a significant part of the ortho-nitrotoluene reaction (25% and 70%, respectively) takes place through an as-yet unspecified process.

B. Trinitro Compounds: Decomposition to Yield Low Molecular Weight Products

Using as background the measured decomposition pathways and rates of mono- and dinitrocompounds discussed above, we conducted preliminary studies of the decomposition of trinitroaromatics using the GC-monitored laser pyrolysis system (LPHP-2 described in detail in Appendix A and reference 1). Preliminary results indicate that the decomposition rate of TNT is similar to that for o-nitrotoluene. The surprising, and as yet unexplained, result is that gas-phase decomposition of TNT does not produce any 2,4-DNT, the

expected product of loss of one of the ortho-nitro groups followed by scavenging of the 2,4-dinitro radical thus produced.



This result applies whether or not a scavenger is present. Not only is DNT absent, but also there are no products in the boiling point range of either mono- or di-nitro compounds. What we do see are products eluting in the vicinity of  $C_2$  or  $C_3$  hydrocarbons, and such products account for at least 50% of the decomposed TNT.

Mass spectral identification of these products has thus far been hindered by limited intensity of the product signals and an interfering background at low mass arising from the large excess of  $SiF_6$  and  $CO_2$ , which elute in the same vicinity. The products might be acetylene derivatives resulting from destruction of the aromatic ring. These could be produced by high temperature decomposition of adsorbed (and infrared absorbing) materials on the KCl windows. Experiments are pending to test this and other possibilities, and thus an extensive discussion is premature. However, because reaction at (or on) the window surfaces is the one possibility for heterogenous reaction that the LPHP-2 system does not preclude, that possibility must always be kept in mind. Therefore, we consider below some factors indicating that reaction at the window surfaces is unimportant.

The first factor that tends to make window reactions unimportant is that reaction times on the order of 10  $\mu s$  are much shorter than diffusion times to the reactor windows for all but that portion ( $\sim 1\%$ ) of the reactants in the laser-heated region closest to the windows. In addition, the windows, because of their low absorption and high heat capacity, are very cold compared with the gas phase reaction temperature. Thus, if the bulk of the substrate residing in the region swept out by the laser beam is, in fact, in the gas phase, then it is probable that the decomposition occurs entirely in the gas phase. Even if, in the case of a low volatility substrate like TNT, there is an equal amount of substrate residing on the

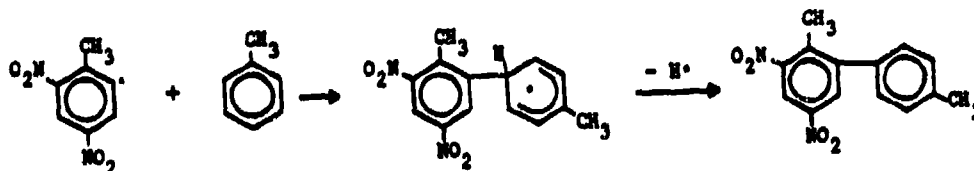
windows as in the gas phase, and even if its extinction coefficient at  $10.6\ \mu\text{m}$  were high enough to heat it to reaction temperature, good thermal contact with the bulk KCl would ensure a heat loss rapid enough to prevent reaction of the adsorbed molecules.

An exception to this generalization could occur if a char coating forms on the KCl surface, which is IR-absorbing, and furthermore is not in good thermal contact with the surface. In this event, any substrate adsorbing on this char could well be heated to temperatures of 2000 K. Such temperatures could generate acetylene derivatives from many different organic substrates. To assess the potential importance of this mode of surface reaction, it is helpful to consider the time dependence of any char formation on the windows. Our observations support the expectation that the formation of such carbon deposits on the windows is an autoacceleratory process: the bigger the carbon particles are, the more substrate and light they can adsorb, the longer they stay hot, and the faster they will grow.

In the case of the mono- and dinitro aromatics, there was no problem with carbon deposits. Such deposits would sometimes form, but only as a small side-reaction and only after weeks of continuous use of the system; more importantly, data taken shortly before the laser heating of the carbon particles became visible to the naked eye showed the same products and rates as data taken weeks earlier. Given the autoacceleratory nature of the carbon formation, this strongly suggests that neither set of data was significantly influenced by surface reactions. In the case of TNT, the carbon deposits form more readily than with the mono- and dinitrotoluenes, but the exclusive production of light products is a result that appears, nevertheless, to be independent of the time remaining before carbon formation is visible.

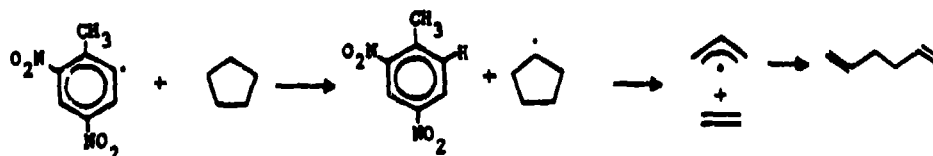
A particular characteristic of nitro-phenyl radicals that could lead to secondary pyrolysis on the windows is an initial formation of less volatile products than otherwise expected from an initial phenyl- $\text{NO}_2$  scission; this occurs because of the tendency of the radicals thus formed to add to the aromatic system of a potential scavenger rather than to abstract benzylic hydrogens. Literature data<sup>6</sup> show that in solution this tendency increases as the number of  $\text{NO}_2$  groups on the phenyl ring increases. In the case of

TNT, this would result in the initially formed 2,4-dinitrophenyl radical adding to toluene to produce a dinitrobiphenyl species.



Whereas TNT has sufficient volatility to remain largely in the vapor phase under LPHP-2 conditions, the biphenyl derivative would have substantially lower volatility. (In the absence of any added scavenger, the initially formed radical could add to TNT itself to produce a tetra- or penta-nitro biphenyl derivative. If these additives were preferentially adsorbed on the KCl surfaces irradiated by the laser rather than on the larger area of non-window surfaces in the cell), further pyrolysis in subsequent laser pulses could account for the good yield of light products.

To determine the possible importance of this addition mode of scavenging, we used cyclopentane rather than toluene as a scavenger. (No addition is possible with cyclopentane.) Cyclopentane functions as a scavenger as indicated below and provides no aromatic system to which a product radical could add.



When TNT was pyrolyzed in the presence of a large excess of cyclopentane, the same low molecular weight products were observed. Thus, radical addition to scavenger molecules does not appear to account for the absence of volatile products from the decomposition of TNT. Furthermore, the complete absence of heavy products in the presence of a large excess of cyclopentane would appear to rule out any chance that dinitrophenyl radicals add to TNT itself. Such self-addition reactions are suggested by the fact that

condensed-phase TNT decomposition is well known to result in formation of materials described<sup>5a</sup> as "explosive coke." This clearly indicates a tendency of some intermediates to undergo addition reactions.

On balance, it does not appear that the failure to see products in the molecular weight range of DNT is merely a result of our inability to scavenge the initially formed radical. This conclusion is supported by the indications (see Appendix) that although o-NT undergoes phenyl-NO<sub>2</sub> bond scission, o-NT itself is very near a threshold for a change in reaction mechanism. Thus, it is possible that the initial series of rapid gas-phase reactions itself result in the destruction of the aromatic ring of TNT and the formation of low molecular weight products. We addressed the question of the role of the methyl group in the exclusive formation of low boiling products by carrying out the decomposition of 1,3,5-trinitrobenzene under the same conditions used for TNT. Only products boiling in the vicinity of C-2 and C-3 hydrocarbons were observed, indicating that a structure having the methyl group flanked by two NO<sub>2</sub> groups is not necessary for facile destruction of the aromatic ring.

In summary, the preliminary results obtained for TNT and TNB do not clearly indicate why there are no products traceable to initial phenyl-NO<sub>2</sub> scission. Although the considerations discussed above suggest that the light TNT products are not the result of surface reaction, definitive evidence one way or the other is needed. To answer this question, we tried raising the cell temperature to the 200-220°C limit of the viton o-rings and covering the laser beam ports with a second set of KCl windows to minimize convectional cooling of the cell windows. These changes resulted in no change in the TNT results (i.e., no observation of volatile products having an intact phenyl ring). This does not rule out loss of vapor-phase products to the walls followed by laser-induced reactions on the window surface, but merely indicates that if any such absorption sequence were taking place, removal of the vapor-phase products from the cell was not even competitive with loss by adsorption.

We plan to take additional, more detailed approaches, including

- (1) Using a longer path-length cell and short focal length mirror to bring the laser beam into the cell, with an intensity sufficient to cause reaction only at the beam waist; this will occur in the center of the cell, remote from the windows.
- (2) Using a longer path-length cell and additional KCl "windows" inside the cell to test the effect of additional KCl surface.

The behavior of the trinitro compounds emphasizes the value, as a complementary technique, of a molecular-beam-sampled version of LPHP, where contact with reactor surfaces is precluded not only during reaction but also before reaction, after reaction, and during detection.

### C. Construction of a Molecular Beam Sampling-Laser Pyrolysis Apparatus (LPHP-3)

#### 1. Vacuum System

The molecular beam (MB) laser pyrolysis system is constructed of 304 stainless steel with two differentially pumped chambers plus a beam dump system, coupled to three oil diffusion pumps, each with Freon-refrigerated baffle (Figure 2). The two first chambers are each evacuated by a 2400 L/s (nominal) NRC pump, the beam dump by a 800 L/s CEC pump. The pumps can be isolated from the chambers by three pneumatic gate valves, automatically activated if overpressure or cooling shutdown is detected. Each pump has its own foreline mechanical pump; foreline pressures are monitored by thermocouple gauges. The second differentially pumped chamber contains an Extranuclear Laboratories 4-324-9 quadrupole mass spectrometer (QMS) with electron impact ionization and perpendicular beam axis disposition. The mass range is 1-50 or 1-400 amu, depending on the high Q-head used. The position of the QMS is adjustable from the outside by three screws and a bellows suspension. Ion current can be detected either by a channeltron or by a simple Faraday cup. The beam dump, placed after the QMS, should collect and trap the residual beam, in order to decrease the pressure in the QMS chamber. The entire pumping system can be degassed by heating up to 200°C. The chamber pressures are monitored with one ion gauge and one thermocouple gauge per chamber, with a fourth ion gauge above the baffle of



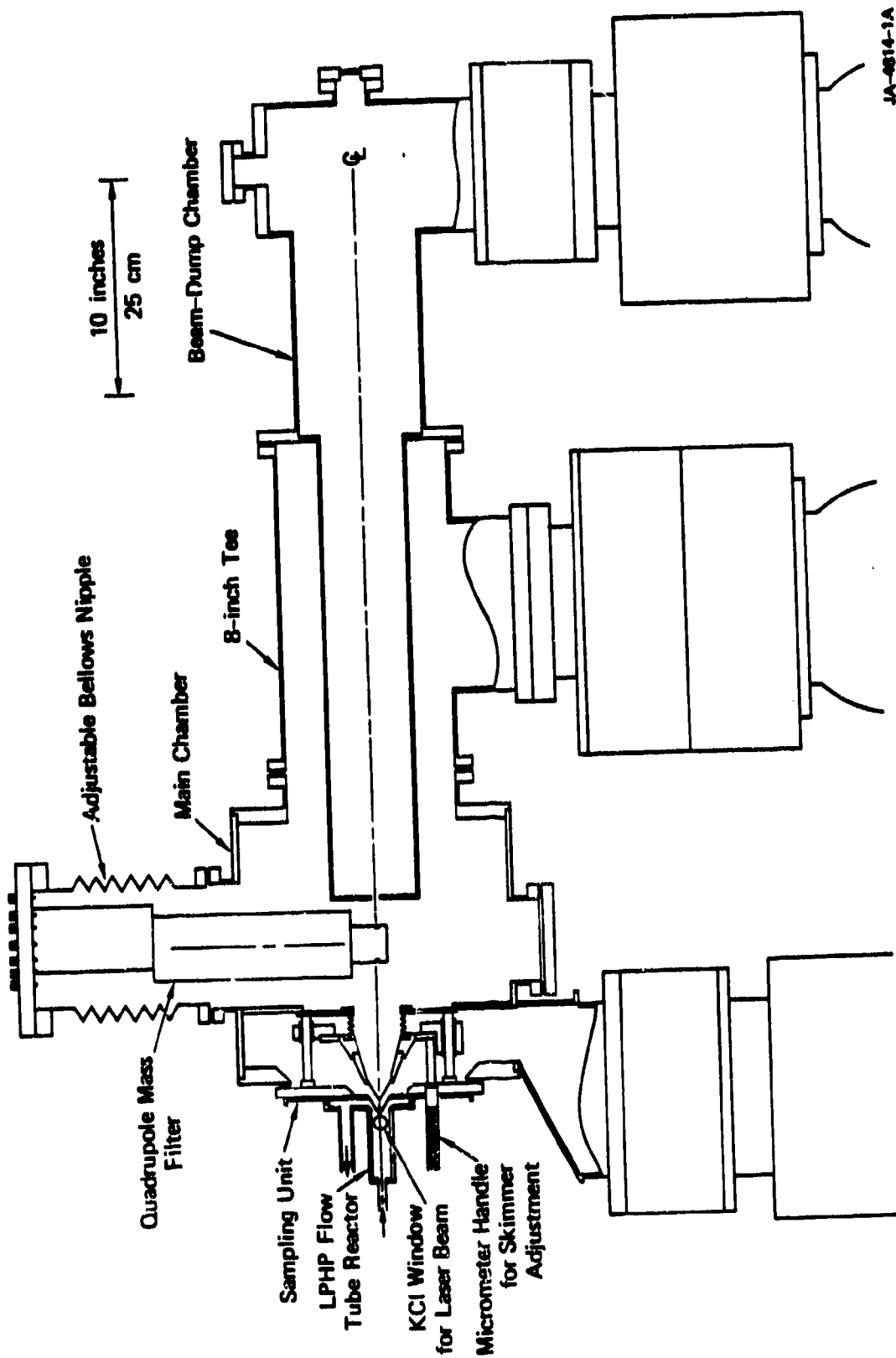


FIGURE 2 ASSEMBLY DRAWING OF THE MOLECULAR-BEAM-SAMPLED, MASS SPECTROMETRICALLY DETECTED LPHP SYSTEM (LPHP-3)

pump No. 2 (QMS chamber). The ultimate pressure (with no beam) is on the order of  $2-3 \times 10^{-8}$  torr in each chamber. The system has been designed to operate with generating pressures up to 100 torr in the flow cell when equipped with a nozzle with a 200- $\mu$ m orifice.

## 2. Flow Cell Operation and MB generation

A skimmer (electroformed nickel, Beam Dynamics, Minneapolis, MN) with 200- $\mu$ m diameter at the throat is used as the supersonic divergent nozzle, with exponential expansion walls. The classical skimmer extracting the central portion of the beam has an input diameter of 200  $\mu$ m. Both the nozzle and the skimmer have attack edges of less than 5- $\mu$ m thickness. The distance between the nozzle and the skimmer entries can be varied from a few millimeters up to 20 mm by external adjustment of a micrometer screw. The nozzle to ionizer distance is 21 cm. Because of the necessity to maintain free access to the laser-heated region in front of the nozzle, this region could not readily be used as a chamber for the first stage of differential pumping. This necessitated a first chamber of some 10-cm thickness, and together with the cross-axis orientation of the quadrupole (needed to avoid deposition of low vapor pressure materials on the quadrupole rods), dictated the total source to ionizer distance. As a consequence, the vacuum system was designed for maximum flexibility and to achieve low background. For instance, should it be desirable, the third chamber, now designated as the beam dump, can be used to provide a separately pumped chamber for the quadrupole and/or to provide for axial placement of the quadrupole head.

The flow cell is a machined aluminum block gas mixing chamber, where  $\text{SF}_6$ , buffer gas, and active material are mixed just before the nozzle. Figure 3 is a schematic drawing of the flow cell; Figures 4 and 5 are photographs of the vacuum chamber with the flow cell separated from the front plate by several inches, revealing the nozzle; and Figure 6 is a photograph of the front plate of the vacuum chamber with the nozzle and its mounting plate removed, revealing the movable skimmer behind it. The cell temperature can be maintained constant to within  $\pm 0.3^\circ\text{C}$ , so as to maintain a constant vapor pressure of nitramine or other substrate. The present limit on the flow cell temperature is set by use of viton o-rings, but this can be

- a. Carrier gas inlet
- b. Dilution gas inlet
- c. Flow cell pumpout
- d. Well(s) for cartridge heater and thermocouple
- e. Substrate reservoir
- f. Retaining ring and shroud for KCl windows
- g. Location of sampling nozzle

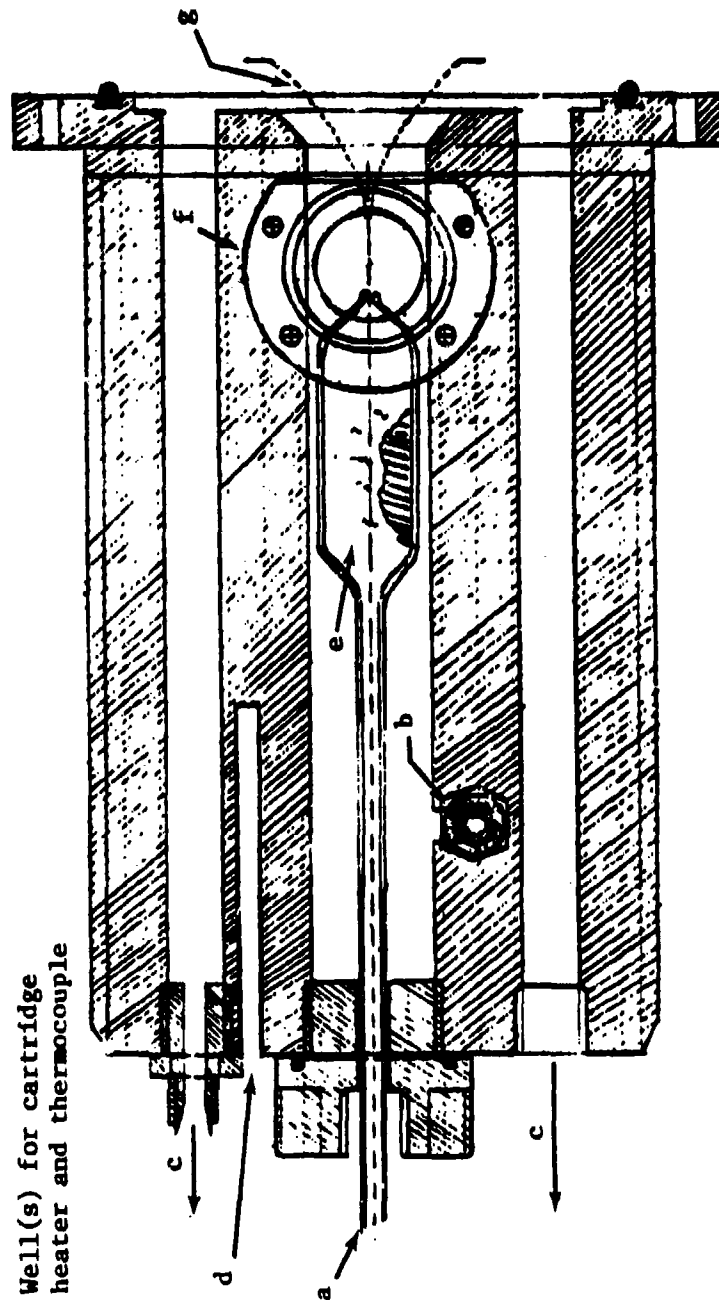
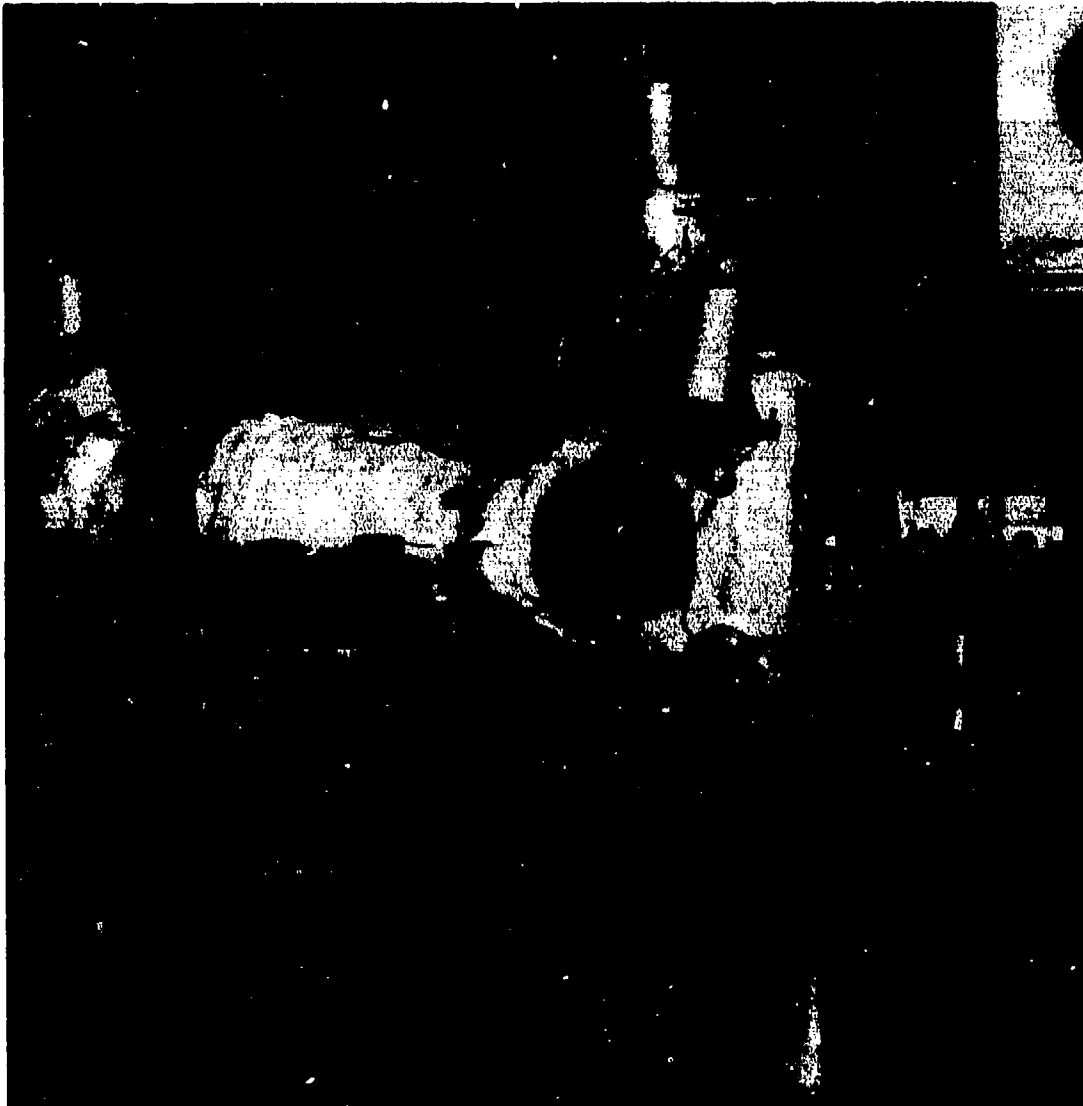


FIGURE 3 SCHEMATIC DRAWING OF MACHINED ALUMINUM FLOW CELL



**FIGURE 4 LPHP-3 VACUUM SYSTEM WITH DISMOUNTED FLOW CELL**



FIGURE 5 CLOSEUP OF NOZZLE AND DISMOUNTED FLOW CELL



FIGURE 6 LPHP-3 VACUUM SYSTEM WITH NOZZLE AND NOZZLE-MOUNTING PLATE REMOVED

increased by the use of other materials if desirable. The cell is designed to operate at flow rates that ensure complete renewal of the gaseous reaction mixture before the next laser heating pulse.

$\text{SF}_6$  and the buffer gas are premixed from commercial cylinders at known partial pressures by controlling pressure and flow using conventional techniques in a vacuum manifold connected to the flow cell. The pressure is reduced from 5 psig to 100 torr by an additional pressure regulator, and about 90% of the flow called the dilution flow is allowed to enter the heated flow cell directly. About 10% of the flow is diverted before the pressure drop to 100 torr; after separate pressure drop to 100 torr and flow measurement, this secondary flow is conducted through a glass tube containing the active substance (HMX, etc., sample flow). This "reservoir" tube extends into the heated flow cell through an o-ring-sealed Cajon fitting. In this manner, small amounts of the active, low vapor pressure substrates are injected into the main, or dilution, flow. The position of the injecting orifice can be adjusted so that mixing of the sample and dilution flows takes place just in front of the laser-irradiated region or several centimeters upstream. In the former case, the substrate in the narrow conical portion of the laser-heated cylinder that is expanded into the nozzle will not have contacted any metal surfaces, either before or after the laser pulse.

The laser beam irradiates the reaction mixture as close as possible to the nozzle, so that the expansion wave generated by the laser heating pushes the gas inside of the expanding nozzle. Thus, a few  $\mu\text{s}$  after the laser pulse, the mixture is frozen by the adiabatic expansion, and radicals formed in the early process of decomposition are transported, without undergoing collision, to the QMS in less than a ms.

## **PARTICIPATING SCIENTIFIC PERSONNEL**

**The following staff contributed to this project:**

**Dr. Donald F. McMillen**

**Dr. David M. Golden**

**Dr. John R. Barker**

**Present address: Department of  
Atmospheric and Oceanic Science  
University of Michigan, Ann Arbor**

**Dr. Alicia C. Gonzalez**

**Visiting Scientist on leave from  
Consejo Nacional de Investigaciones  
Cientificas de la Republica Argentina**

**Dr. C. William Larson**

**Present address: AFRL/LKCS  
Edwards AFB, CA**

## SUMMARY

Laser-powered homogenous pyrolysis has been successfully used to provide conditions where surface-sensitive and strongly adsorbing substrates can be indirectly heated by an infrared laser and allowed to react while remote from potentially catalytic surfaces. Furthermore, the use of internal temperature standards allows the "effective" reaction temperature to be defined such that accurate Arrhenius parameters for the homogeneous gas-phase decomposition can be determined. Application of the technique to the decomposition of the mono-, di-, and tri-nitro benzenes has allowed the determination of the Arrhenius parameters for the respective phenyl-NO<sub>2</sub> bond scission reactions, even in the case of two ortho-methyl substituted nitrobenzenes (ortho-nitrotoluene and 2,4-dinitrobenzene). All previous attempts to determine the homogeneous gas-phase decomposition pathways for these nitrobenzenes had failed apparently because of their proclivity for surface-catalyzed processes.

The homogenous gas-phase decomposition behavior of the mono-nitrobenzenes has turned out to be less simple than anticipated: The effect of an ortho-methyl group is sufficient not only to significantly accelerate the expected loss of an adjacent -NO<sub>2</sub> group, but also to open up a new reaction pathway. Thus, even under "truly" homogeneous gas-phase reaction conditions, a minor fraction of the reaction proceeds through a pathway that does not produce the o-methylphenyl radical expected from phenyl-NO<sub>2</sub> bond scission. In general agreement with these results are preliminary results obtained by Tsang in a heated single-pulse shock tube, although the exact rates and the fraction of reaction proceeding by the "abnormal" decomposition are somewhat different. We anticipate that determination of the factors affecting the amount of abnormal reaction observed will provide a valuable key to understanding the decomposition pathways in functioning nitroaromatic explosives.



Preliminary studies of trinitrotoluene and trinitrobenzene exhibit what may be an extension of the behavior of ortho-nitrotoluene, in that no products reflecting initial phenyl-NO<sub>2</sub> bond scission could be detected, and substantial amounts of low molecular weight gases were observed. There are indications that this fragmentation of the aromatic ring is actually a homogeneous gas-phase reaction; however, experimental results do not at this point allow us to rule out formation, from the tri-nitro aromatics, of intermediate addition compounds having too low a vapor pressure to escape from the cell. Adsorption of these materials on the inner surfaces of the KCl windows could then result in pyrolysis of the adsorbed materials at temperatures high enough to cause fragmentation of any aromatic ring.

The recently completed molecular-beam mass-spectrometrically monitored version of LPHP (LPHP-3) is expected to be particularly valuable in clarifying this behavior of the tri-nitroaromatics and other energetic materials of very-low vapor pressure. The capability for direct, real-time observation of the initial fragments will be highly complementary to the GC/MS-monitored LPHP-1 that is limited to analysis of a scavenged product mixture, but whose capability to quantitate complex reaction mixtures with an extremely wide dynamic range makes it well-suited to the measurement of rate parameters over a wide temperature range. We are currently testing out the LPHP-3 system; we are also adding to the original pulsed laser heating source a cw laser-heating capability that will facilitate separation of chemical reaction effects from the gas-dynamic heating effects and will also substantially increase the duty cycle of the system.

In summary, the LPHP technique, as already embodied in the well-mixed-reactor, GC/MS-monitored version, has provided rate and mechanistic information on the homogeneous gas-phase decomposition of moderate molecular weight, low vapor-pressure, surface-sensitive nitroaromatics that was not previously available from other techniques. Use of the recently completed LPHP-3 will make identification of initial decomposition products more direct and also extend the capability to materials of substantially lower vapor pressures. Together these techniques will help provide an information base of the intrinsic decomposition behavior of energetic materials that is necessary for understanding the chemical factors that control the decomposition of functioning condensed-phase energetic materials.

#### REFERENCES

1. D. F. McMillen, K. E. Lewis, G. P. Smith, and D. M. Golden, J. Phys. Chem., 86, 709 (1982).
2. W. Tsang, personal communication, December 1985.
3. H.-L. Dai, E. Specht, M. R. Berman, and C. B. Moore, J. Chem. Phys., 77, 4494 (1982).
4. W. Tsang, Chem. Phys., 41, 2487 (1964).
5. See, for example:
  - (a) J. C. Dacons, H. G. Adolph, and M. J. Kamlet, J. Phys. Chem., 74, 3035 (1970).
  - (b) V. G. Matveev, V. V. Dubikhin, and G. M. Nazin, Inst. Khim. Fiz. Chronogolovka, USSR, 4, 783 (1978).
  - (c) V. G. Matveev, V. V. Dubikhin, and G. M. Nazin, Acad. Sci., USSR Bull., Div. Chem. Sci., 2, 474 (1978), and references cited therein.
6. W. A. Pryor, F. Y. Yang, R. H. Tang, and D. F. Church, J. Am. Chem. Soc., 104, 2885 (1982).

**Appendix A**

**MECHANISM OF DECOMPOSITION OF NITROAROMATICS:  
LASER-POWERED HOMOGENEOUS PYROLYSIS OF SUBSTITUTED NITROBENZENES**

**by**

**Alicia C. Gonzalez, C. William Larson,  
Donald F. McMillen, and David M. Golden**

**The Journal of Physical Chemistry, 1985, 89, 4809**

# Mechanism of Decomposition of Nitroaromatics. Laser-Powered Homogeneous Pyrolysis of Substituted Nitrobenzenes

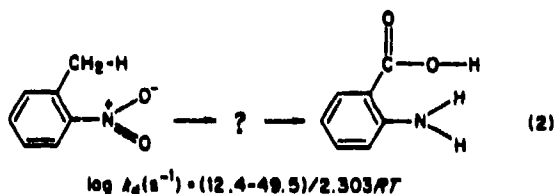
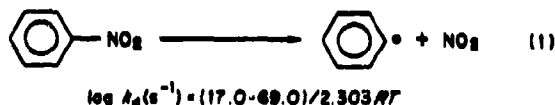
Alicia C. Gonzalez,<sup>†</sup> C. William Larson,<sup>‡</sup> Donald F. McMillen,\* and David M. Golden

Department of Chemical Kinetics, Chemical Physics Laboratory, SRI International,  
Menlo Park, California 94025 (Received: December 26, 1984)

Laser-powered homogeneous pyrolysis (LPHP) has been used to study the gas-phase thermal decomposition of nitrobenzene (NB), *m*-dinitrobenzene (*m*-DNB), *p*-nitrotoluene (*p*-NT), *o*-nitrotoluene (*o*-NT), and 2,4-dinitrotoluene (2,4-DNT) under conditions where surface-catalyzed reactions are precluded. The Arrhenius parameters have been determined by comparative rate measurements relative to cyclohexene decomposition and the reaction mechanisms have been established. In all cases, the rate-limiting step is the homolysis of the Ar-NO<sub>2</sub> bond. The measured Arrhenius parameters for homolysis range from  $\log A = 14.5$  to  $16.4$  and  $E_a$  from  $67.0$  to  $70.0$  kcal/mol. The C-NO<sub>2</sub> bond dissociation energies (kcal/mol) and values of  $\log k$  (s<sup>-1</sup>) for NB, *m*-DNB, *p*-NT, *o*-NT, and 2,4-DNT have been derived from these results and are as follows:  $71.4 \pm 2.0$ ,  $(15.5 \pm 0.5) - (68.2 \pm 1.7)/2.3RT$ ;  $73.2 \pm 2.4$ ,  $(14.5 \pm 0.5) - (70.0 \pm 2.1)/2.3RT$ ;  $71.4 \pm 2.3$ ,  $(14.9 \pm 0.5) - (68.2 \pm 2.0)/2.3RT$ ;  $70.2 \pm 2.5$ ,  $(16.4 \pm 0.6) - (67.0 \pm 2.2)/2.3RT$ ;  $70.6 \pm 2.0$ ,  $(15.3 \pm 0.4) - (67.4 \pm 1.7)/2.3RT$ .

## Introduction

The thermal decomposition of aromatic nitrocompounds has received considerable attention from chemists over the last 50 years, but the reported<sup>1</sup> Arrhenius parameters cover a wide range and the products of the initial steps are essentially unknown. It is well-known<sup>2</sup> that the thermal decomposition of nitrobenzene in a N<sub>2</sub> carrier stream results in biphenyl and other products traceable to initial bond scission to form phenyl radical and NO<sub>2</sub>, but *o*-nitrotoluene reacts under these same conditions by a different pathway.<sup>3</sup> In the latter case, the principal product has been shown to be aniline, resulting from the initial formation of anthranilic acid.<sup>3</sup> Similarly, the presence of an *o*-methyl, -amino, or -hydroxy substituent has been reported<sup>4</sup> to cause a shift in the Arrhenius parameters for gas-phase decomposition from those expected for thermolysis of an approximately 70 kcal/mol bond to values suggestive of a complex intramolecular process:



Although various six-membered transition states leading to the intramolecular redox reaction shown in reaction 2 are geometrically quite plausible, none of them appear to lead directly to sufficiently stable products to be associated with the observed activation energy: OH elimination has been suggested<sup>4</sup> as the first step, but this reaction as written is estimated<sup>5</sup> to be 80 kcal/mol endothermic, and therefore could not give rise to an activation energy in the range of 40 kcal/mol. On the other hand, the stable products observed in reaction 2 require substantial movement of at least four atoms, a kind of rearrangement that is difficult to imagine taking place in a single elementary step in the gas phase. These results lead us to suggest that the complex reactions indicated by the reaction products and the unexpectedly low Arrhenius parameters were due to surface-catalyzed reactions, notwithstanding efforts made to avoid them. This would be consistent with various condensed-phase TNT studies that have

suggested through spectroscopic observations<sup>6</sup> or isotope effects<sup>7</sup> that the initial reaction(s) do involve the *o*-methyl group.

Preliminary experiments in which very low-pressure pyrolysis (VLPP) was used to study the decomposition of 2,4-dinitrotoluene also provide rates consistent with a low  $A$  factor and low activation energy process ( $\log k_1$  (2,4-DNT) (s<sup>-1</sup>) =  $(12.1 - 43.9)/2.3RT$ ), and not indicative of thermolysis of the Ar-NO<sub>2</sub> bond.<sup>8</sup> Since in VLPP all substrate heating is by contact with the reactor walls, surface-catalyzed reactions can dominate in substrates that are prone to them. Therefore, various coatings were used on the VLPP reactor in attempts to eliminate such reactions, but ultimately what appeared to be a surface-catalyzed reaction could not be eliminated. Thus these results were consistent with, but did not prove, our speculation that the low Arrhenius parameters previously reported were due to surface reactions.

We have developed a pulsed-laser technique in which a CO<sub>2</sub> laser is used to indirectly heat the substrate via an absorbing but unreactive gas (e.g., SF<sub>6</sub>). During and after the laser heating of the SF<sub>6</sub>, rapid vibrational-to-vibrational energy transfer occurs between SF<sub>6</sub> and the bath and sample molecules. Under these conditions, there is no surface component to the reactions, since the wall remains cold relative to the reaction temperature. After

- (1) (a) Dacons, J. C.; Adolph, H. G.; Kamlet, M. J. *J. Phys. Chem.* 1970, 74, 3035. (b) See, for example: Makimov, Y. Y. *Russ. J. Phys. Chem.* 1972, 46, 990. Dubovitskii et al. *Ibid.* 1961, 35, 148. (c) Beckmann, J. W.; Wilkes, J. J.; McGuire, R. P. *Thermochim. Acta* 1977, 19, 111.
- (2) Hand, C. W.; Merritt, Jr., C.; DiPietro, C. J. *Org. Chem.* 1977, 42, 841.
- (3) (a) Fields, E. K.; Meyerson, S. *Tetrahedron Lett.* 1968, 10, 1201. (b) Fields, E. K.; Meyerson, S. *Adv. Free-Radical Chem.* 1968, 5, 101.
- (4) (a) Matveev, V. G.; Dubikhin, V. V.; Nazin, G. M. *Inst. Khim. Fiz. Chronologika, USSR* 1978, 4, 783. (b) Matveev, V. G.; Dubikhin, V. V.; Nazin, G. M. *Acad. Sci., USSR Bull., Div. Chem. Sci.* 1978, 2, 474 and references cited therein.
- (5) (a) Benson, S. W. "Thermochemistry and Chemical Kinetics", 2nd ed.; Wiley: New York, 1976. (b) McMillen, D. F.; Golden, D. M. *Annu. Rev. Phys. Chem.* 1982, 33, 493-532. (c) Batt, L.; Robinson, G. N. In "Chemistry of Functional Groups - Supplement F"; Patai, S., Ed.; Wiley: Chichester, UK, 1981; p R1035.
- (6) (a) Davis, L. P.; Turner, A. G.; Carper, W. R.; Wilkes, J. S.; Dorey, R. C.; Pugh, H. L.; Siegenthaler, K. E. 181st National Meeting of the American Chemical Society, Atlanta, Ga, March-April 1981; American Chemical Society: Washington, DC, 1981. (b) Sharma, J.; Owens, F. J. *Chem. Phys. Lett.* 1979, 61, 280. Owens, F. J.; Sharma, J. *J. Appl. Phys.* 1980, 51, 1494. (c) Davis, L. P.; Turner, A. G. *Int. J. Quantum Chem.* 1983, 17, 193. (d) Turner, A. G.; Davis, L. P. *J. Am. Chem. Soc.* 1984, 106, 5447. (e) Davis, L. P.; Turner, A. G.; Carper, W. R.; Wilkes, J. S.; Dorey, R. C.; Pugh, H. L.; Siegenthaler, K. E. "Thermochemical Decomposition of TNT: Radical Identification and Theoretical Studies"; Frank J. Seiler Research Laboratory, Project Report FJSRL 1R-81-0002, April 1981.
- (7) Shackelford, S. A.; Beckman, J. W.; Wilkes, J. S. *J. Org. Chem.* 1977, 42, 4701.
- (8) McMillen, D. F., unpublished work.

<sup>†</sup> Visiting Scientist on leave from Consejo Nacional de Investigaciones Científicas de la República Argentina.

<sup>‡</sup> Currently at Rocket Propulsion Laboratory, Edwards Air Force Base, CA.

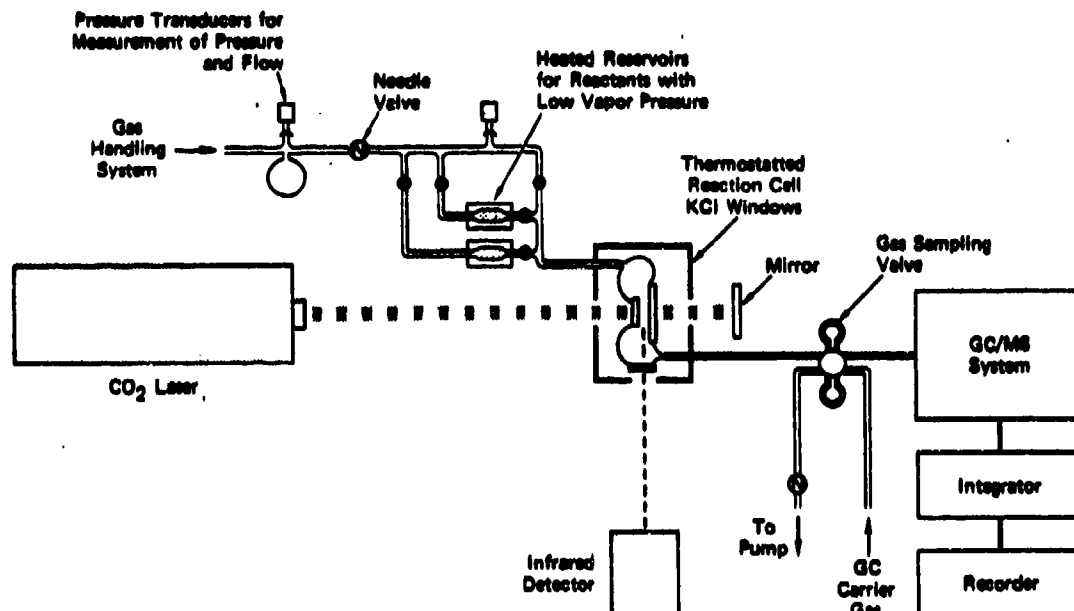


Figure 1. Schematic of gas chromatographically monitored laser-powered homogeneous pyrolysis flow system.

a sufficient number of these collisions, thermal equilibrium is attained, and observed reaction rates reflect thermal Arrhenius parameters. IR fluorescence measurements show that the entire mixture is brought to temperature in less than  $3 \mu\text{s}$  and that the reaction time before cooling by an expansion wave is about  $10 \mu\text{s}$ , far shorter than the millisecond time scale for diffusion to the walls. The heated flow system we have incorporated<sup>9</sup> makes this technique suitable for studying substrates (like the nitroaromatics) with very low vapor pressure at room temperature. This enables us to study the decomposition of the nitroaromatics under conditions where the rates and products of the initial step can be measured, and where a clear distinction can be made between homogeneous gas-phase processes and those processes aided by association with surfaces or condensed phases.

#### Experimental Section

Figure 1 shows a schematic of the LPHP flow system, which is described in detail elsewhere.<sup>9</sup> A slow flow of  $\text{SF}_6$  (infrared absorber),  $\text{CO}_2$  (inert collider), temperature standard (cyclohexene), radical scavenger (*o*-fluorotoluene or cyclopentane), and substrate were passed through the reaction cell, through a heated gas chromatographic sampling valve, through a needle valve, and into a vacuum pump. The flow line and the reactor were heated to  $100^\circ\text{C}$ , to avoid condensation problems. Flow was maintained at the desired level by adjusting the first needle valve and total pressure was maintained at 110 torr by adjusting the second needle valve. A small portion of the reaction cell (typically 2–5%) was irradiated with the P20 line  $\lambda = 10.6 \mu\text{m}$  of a Lumonics K103  $\text{CO}_2$  laser (duration =  $1 \mu\text{s}$ , fluence =  $1 \text{ J}/\text{cm}^2$ ) at a constant repetition rate (0.2 Hz) until a new steady state of products and undecomposed substrate was attained as shown schematically in Figure 2. The cell incorporates KCl windows to transmit the IR radiation, a  $1.2\text{-cm}^2$  laser aperture to define the heated volume, and a rear reflecting mirror to maintain axial temperature homogeneity under conditions where as much as 20% of the laser radiation is absorbed in a single pass. The reaction temperature was controlled by varying the IR radiation energy and the  $\text{SF}_6$  content of the gas mixture. The flow time and irradiation frequency provide at least 20 laser shots during the average flow lifetime of a substrate molecule in the cell and ensure complete gas mixing between shots.

When the system reaches the "steady-state" with the laser being repeatedly pulsed, the decrease in average concentration of sub-

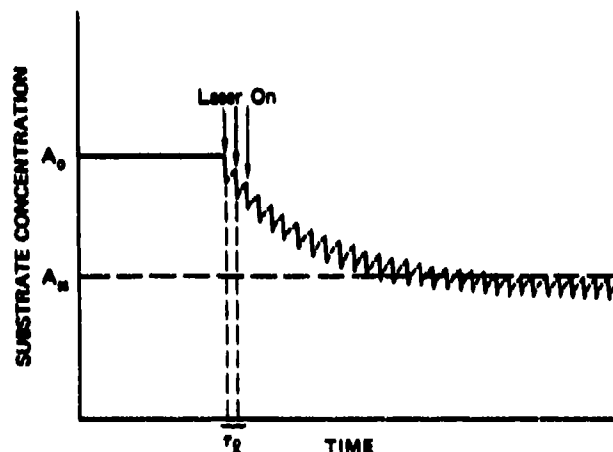


Figure 2. Schematic representation of a spatially averaged substrate concentration as a function of time.

strate  $A$  during any single laser pulse equals the replenishment (by flow) of  $A$  before the next laser pulse and results in the sawtooth horizontal line shown in Figure 2. Under these conditions, measurements of the average fractional decomposition lead to the rate constant for substrate decomposition via eq 1

$$k\tau_r \approx -\ln \left[ 1 - \left( \frac{[A]_0}{[A]_m} - 1 \right) \frac{V_T}{V_R} \left( \frac{\tau_l}{\tau_r} \right) \right] \quad (1)$$

where  $k$  is the first-order rate constant describing disappearance of  $A$ ,  $\tau_r$  is the reaction time ( $10 \mu\text{s}$ ) following each laser pulse,  $\tau_l$  is the time between laser pulses (4 s),  $\tau_f$  is the flow lifetime in the reaction cell (typically 200 s),  $V_T$  and  $V_R$  are the total and laser-heated cell volumes, and  $A_0$  and  $A_m$  are the laser-off and laser-on steady-state substrate concentrations, respectively.<sup>9</sup>

The need to measure explicitly the temperature corresponding to any particular measurement of  $k$  is eliminated by concurrent determination of the fractional decomposition of a temperature standard, a second substrate whose decomposition rate temperature dependence is already well-known, and therefore whose fraction decomposition defines an "effective" temperature.<sup>9</sup>

$\log k_1\tau_r =$

$$\log A_1 + \left( 1 - \frac{E_1}{E_2} \right) \log \tau_r - \frac{E_1}{E_2} \log A_2 + \frac{E_1}{E_2} \log k_2\tau_r \quad (11)$$

(9) McMillen, D. F.; Lewis, K. E.; Smith, G. P.; Golden, D. M. *J. Phys. Chem.* 1983, 86, 709.

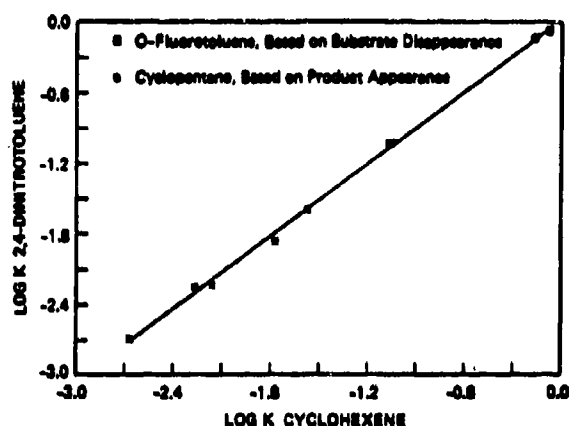


Figure 3. Effect of scavenger on 2,4-dinitrotoluene decomposition rate.

According to eq II, a plot of  $\log k_1$  vs.  $\log k_2$  gives a straight line of  $\log k_1 = \text{slope } E_1/E_2$  and intercept of

$$\log A_1 + [1 - (E_1/E_2)] \log \tau_r - [E_1/E_2] \log A_2$$

Inspection of eq II reveals that uncertainties in reaction times will cause no error in the slope of the comparative rate plot (the measured activation energy) and that the error in the intercept ( $A$  factor) will be given by  $[1 - (E_1/E_2)] \log (\tau_{r, \text{std}}/\tau_{r, \text{unk}})$ . When  $E_1$  and  $E_2$  are not greatly different, this error will be insignificant. For example, when  $E_1/E_2 = 0.9$ , even a tenfold error in  $\tau_{r, \text{std}}$  will result in an error in  $\log A_{\text{unk}}$  of only 0.1 log units. This is in accord with the error analyses for the comparative rate technique as applied to the single-pulse shock tube.<sup>9,10</sup>

The comparative rate technique is similarly accommodating with respect to variations of temperature with time and space within the laser-heated volume. Under the conditions described above, and when the activation energy of the standard is within  $\sim 5$  kcal/mol of the unknown, and when the fractional decomposition of both unknown and standard are maintained below  $\sim 20\%$  per shot in the laser-heated volume, error analyses<sup>9,11</sup> and tests with "dummy" unknowns have shown<sup>9</sup> that the systematic error is less than  $\sim 1$  kcal/mol, irrespective of the range of the temperature variations. In other words, for suitably matched unknown and temperature standard, temperature variations will be tracked very similarly by the unknown and the standard. In the limit of exact Arrhenius parameter match, of course, there will be no systematic error.

Cyclohexene was chosen as the temperature standard because of its very well-known kinetic parameters, the stable products it forms, and also because its activation energy was close to the expected activation energies for the nitrocompounds.

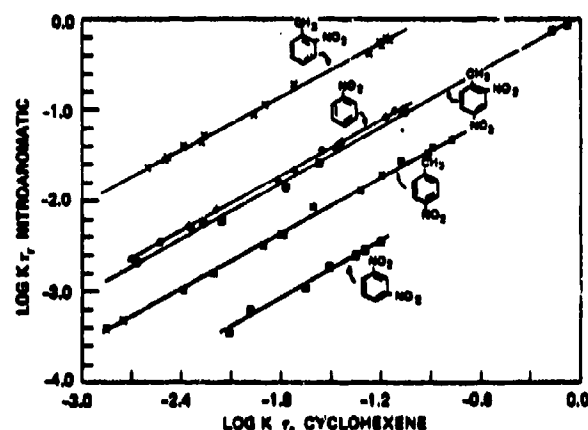


$$\log k \text{ (s}^{-1}\text{)} = (15.15 - 66.6)/2.3RT$$

In all the experiments the products have been identified by using a GC equipped with a mass-selective detector (Hewlett Packard 5880 A and 5970 A) and the average concentrations of reactant and products were measured gas chromatographically by using a flame ionization detector.

## Results

For all of the nitroaromatics studied here the principal reaction pathway, as will be seen, involved scission of Ar-NO<sub>2</sub> bond to form, after radical scavenging, the corresponding Ar-H. Initial experiments, conducted without a radical scavenger, showed several secondary products in small amounts, so that the use of a scavenger to react with the radicals formed in the first step was necessary.

Figure 4. LPHP comparative rate plot for ArNO<sub>2</sub> decomposition.TABLE I: LPHP Derived Arrhenius Parameters of Ar-NO<sub>2</sub> Decomposition

compd	$\log A_1$	$E_1$
NB <sup>a</sup>	$15.2 \pm 0.4$	$66.5 \pm 1.5$
<i>m</i> -DNB <sup>a</sup>	$14.5 \pm 0.5$	$70.0 \pm 2.1$
<i>p</i> -NT <sup>a</sup>	$14.8 \pm 0.5$	$67.8 \pm 2.0$
<i>o</i> -NT <sup>a</sup>	$15.9 \pm 0.5$	$65.5 \pm 2.0$
2,4-DNT <sup>a</sup>	$15.2 \pm 0.4$	$67.0 \pm 1.5$
NB <sup>b</sup>	$15.2 \pm 0.4$	$67.2 \pm 1.5$

<sup>a</sup> Rate parameters for total rate of Ar-NO<sub>2</sub> disappearance; the difference between these values and those for bond scission only is experimentally insignificant (i.e.,  $\Delta \log A \leq 0.04$ ). <sup>b</sup> Rate parameters for ArH formation only.

To choose the optimum amount of scavenger, several runs were made in the presence of *o*-fluorotoluene or cyclopentane up to a 400/1 ratio to the nitroaromatic concentration. When ratios greater than 50/1 were used, the system did not show any change in the reaction rate or in the product distribution. A ratio greater than 100/1 was usually used. Figure 3 shows a comparative rate plot for 2,4-DNT decomposition with *o*-fluorotoluene or cyclopentane as the radical scavenger, illustrating that the rate constants are independent of the identity of the scavenger.

Although small flow variations and low fractional decomposition make an exact mass balance difficult to establish, in only one case did the sum of all detected products leave more than 5–8% of the decomposed starting material unaccounted for. This was for *o*-nitrotoluene, where the mass balance ranged between 75 and 80%. Figure 3 shows a comparative rate plot for 2,4-dinitrotoluene that is based on starting material disappearance and product appearance, illustrating the good mass balance.

The comparative rate data plots for the decomposition of nitrobenzene to form benzene (75–80% yield based on the NB decomposed) and phenol (20–25%), *o*- and *p*-nitrotoluene to form toluene (70–95%) and *o*- and *p*-cresol, respectively (7–8%), 2,4-dinitrotoluene to form *p*-nitrotoluene and small amounts of *o*-nitrotoluene (8%), and *m*-dinitrobenzene to form nitrobenzene and small amounts of benzene are all shown in Figure 4.

The Arrhenius parameters ( $k_{\text{un}}$ ) are obtained from the data in Figure 4 by using the comparative rate expression shown above (eq II). Since under the present conditions ( $p = 320\text{--}375$  torr and  $T = 1100\text{--}1250$  K), the cyclohexene decomposition is very slightly in the falloff ( $k_{\text{un}}/k_{\infty} = 0.96\text{--}0.99$ ), the temperature dependence does not correspond exactly to the high-pressure Arrhenius parameters. In order to determine the temperature dependence of cyclohexene at this degree of falloff, we performed a RRKM calculation using a collision efficiency of  $\beta = 0.1\text{--}0.09$  and a transition-state model in which the motion of the separating fragments are treated as loosened vibrations. From this we derived

$$\log k_{\text{un,CHE}} \text{ (s}^{-1}\text{)} = (14.9 - 65.5)/2.3RT$$

These parameters when coupled to the slope and intercept derived

(10) (a) Tsang, W. J. *Chem. Phys.* 1964, 40, 1171. (b) Tsang, W. J. *Ibid.* 1964, 41, 2487. (c) Tsang, W. J. *J. Phys. Chem.* 1972, 76, 143. (d) Tsang, W. J. *Ibid.* 1967, 46, 2817.

(11) Dai, H.-L.; Specht, E.; Berman, M. R.; Moore, C. B. *J. Chem. Phys.* 1962, 77, 4494.

TABLE II: Experimental Parameters, Estimated Extents of Falloff, and High-Pressure Parameters for the Thermalolysis of the Ar-NO<sub>2</sub> Bond

compd	log A <sub>i</sub>	E <sub>i</sub>	derived high-pressure parameters		
			k/k <sub>∞</sub>	log A <sub>∞</sub>	E <sub>∞</sub>
NB	15.2 ± 0.4	67.2 ± 1.5	0.84	15.3 ± 0.5	68.2 ± 1.7
1,3-DNB	14.5 ± 0.5	70.0 ± 2.1	(1)	14.5 ± 0.5	70.0 ± 2.1
p-NT	14.8 ± 0.5	67.8 ± 2.0	0.96	14.9 ± 0.5	68.2 ± 2.0
o-NT	15.9 ± 0.5	65.5 ± 2.0	0.75	16.4 ± 0.6	67.0 ± 2.2
2,4-DNT	15.2 ± 0.4	67.0 ± 1.5	0.96	15.3 ± 0.4	67.4 ± 1.7

from the relative rate data plot give us the  $E_i$  and the  $A$  for the nitroaromatics summarized in Table I.

To obtain the high-pressure parameters, the experimental  $k_{uni}$  were fitted via an RRKM calculation using a modified Gorin model for the transition state<sup>12</sup> and literature vibrational assignments for nitrobenzene.<sup>13</sup> In this model the modes of the transition state are taken as the vibration and rotations of the NO<sub>2</sub> and phenyl fragments. The external rotation about the NO<sub>2</sub>-Ph axis is taken as active, and the other two external rotations are taken as adiabatic in the molecule. The internal rotation about the NO<sub>2</sub>-Ph axis is free in the transition state, and the other internal rotations of the phenyl and NO<sub>2</sub> fragments are taken as "restricted" free rotation at the Ph-NO<sub>2</sub> distance of the critical configuration. The degree of restriction is accounted for by the hindrance parameter<sup>12</sup> which ranged from 0.9 to 0.95, which decrease the entropy of the internal rotation by decreasing the effective moment of inertia of the rotor. A temperature-independent value 0.1 was chosen for the collision efficiency  $\beta$ . The results are presented in Tables II and III (virtually identical high-pressure Arrhenius parameters were obtained by fitting the data with a vibrational transition-state model). The changes in the nitrobenzene parameters that resulted from increasing  $\beta$  to 0.15 were negligible, mainly because the system is very close to the high-pressure limit.

For each compound, we found the high-pressure parameters that best reproduced our experimental rate constants in the following way: we arbitrarily chose sets of  $A$  factors ranging from our  $A$  experimental to  $\log A = 17.0$  at 0.5 log unit increments, (the high-pressure  $A$  factor was actually not constant, but was allowed to decrease by  $\log A = 0.1$  from 1100 to 1250 K in order to match experimental curvature in  $\log k$  vs.  $T$ . This corresponds to a slightly temperature-dependent value of the hindrance parameter.<sup>12</sup> We then adjusted  $E_i$  to fit our experimental rate constant at 1100 and 1250 K exactly. Unless the exactly correct  $A$  factors were by chance among those chosen initially, this required slightly different values of  $E_i$  at 1100 and 1250 K for each  $A$  factor. The best in the initially selected set of  $\log A$  values was that which allowed the experimental  $k_{uni}$  to be fit exactly with a minimum difference in  $E_i$  at 1100 and 1250 K. We made the final adjustment by taking an  $E_i$  that is a weighted average of the set of values bracketing the correct  $E_i$  (i.e., the "minimum difference"  $E_i$  set), and with it obtained the high-pressure parameters that exactly reproduce the  $k_{uni}$  experimental at  $T$ .

The question of the uniqueness of the rate parameters and the sensitivity of the fit is addressed by the Arrhenius plot in Figure 5. The solid line is a plot of  $k_{uni}(NB_{expt})$  and also represents almost exactly the RRKM calculated  $k_{uni}$  values obtained for  $\log A_{\infty} = 15.5$  (15.4 at 1250 K and  $E_{\infty} = 68.2$ . For comparison, the dashed  $k_{uni}$  values were calculated for  $\log A_{\infty} = 16.2$  (16.1 at 1250 K). The upper solid line represents  $k_{\infty}$  for the fitted parameters, illustrating the extent of falloff observed under these conditions.

The above results provide convincing evidence that the homogeneous gas-phase thermal decomposition of the aromatic nitrocompounds in the presence of radical scavenger SH proceeds by initial homolysis of the C-NO<sub>2</sub> bond, the weakest in each of the respective substrates, and that the complex intramolecular steps

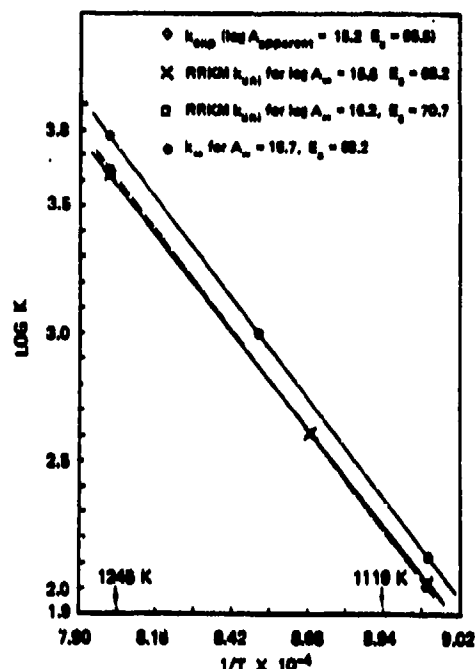
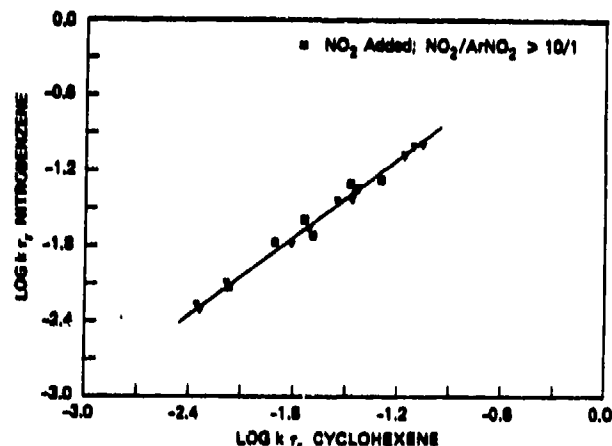


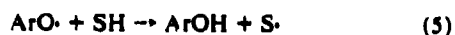
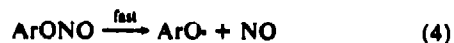
Figure 5. LPHP rate constants and RRKM fittings for nitrobenzene.

Figure 6. Effect of NO<sub>2</sub> addition on nitrobenzene decomposition.

suggested in the literature do not take place as homogeneous gas-phase reactions:



In order to determine whether reaction 1 is reversible (-1) under the LPHP conditions, and to determine whether the observed phenol and cresol formation result from recombination of the NO<sub>2</sub> at the oxygen (-1') followed by reactions 4 and 5 or by an intramolecular rearrangement reaction 3, the decomposition of nitrobenzene was studied in the presence of added NO<sub>2</sub>.



Addition of NO<sub>2</sub> at ratios up to 50/1 NO<sub>2</sub>/NB did not affect either the product distribution or the rate parameters, as is shown in Figure 6. It is clear, therefore, that under the conditions of these experiments no Ar $\cdot$  returns either to ArNO<sub>2</sub> (-1) or to ArONO (-1'), and all observed phenol formation must be the

(12) Smith, G. P.; Golden, D. M. *Int. J. Chem. Kinet.* 1978, 10, 489.

(13) Green, J. H. S.; Harrison, D. J. *Spectrochim. Acta, Part A* 1970, 26A, 1925.

TABLE III: High-Pressure Arrhenius Parameters for Ar-NO<sub>2</sub> Homolysis and Derived BDE Values and Radical Recombination Parameters

compd	log <i>A</i> , s <sup>-1</sup>	<i>E<sub>a</sub></i> , kcal/mol	BDE, <sup>a</sup> kcal/mol	Δ <i>S</i> <sub>‡</sub> <sup>b</sup> , cal/(mol °C)	log <i>A</i> <sub>1100</sub> , s <sup>-1</sup> M <sup>-1</sup>	<i>E</i> <sub>1100</sub> , <sup>c</sup> kcal/mol
NB	15.5 ± 0.5	68.2 ± 1.7	71.4 ± 2.0	45.5	8.6 ± 0.5	1.1
1,3-DNB	14.5 ± 0.5	70.0 ± 2.1	73.2 ± 2.4	42.3	8.4 ± 0.5	1.1
<i>p</i> -NT	14.9 ± 0.5	68.2 ± 2.0	71.4 ± 2.3	42.8	8.7 ± 0.5	1.1
<i>o</i> -NT	16.4 ± 0.6	67.0 ± 2.2	70.2 ± 2.5	49.6	8.7 ± 0.6	1.1
2,4-DNT	15.3 ± 0.4	67.4 ± 1.7	70.6 ± 2.0	42.8	8.7 ± 0.4	1.1

<sup>a</sup> Δ*H*<sub>298</sub><sup>°</sup>. <sup>b</sup> For the sake of consistency, the lower bond scission *A* factors have been taken to imply lower overall entropy decreases for dissociation. This results in a compensation effect, making all log *A*, similar. <sup>c</sup> *E<sub>a</sub>* is for recombination described in concentration units.

TABLE IV: Effect of Substituents

compd	log <i>k<sub>a</sub></i> (1100 K) <sup>a</sup>	ΔBDE, kcal/mol	Δ log <i>k</i>	Δ(Δ <i>G</i> <sup>°</sup> ), kcal/mol
NB	1.93	(0)	(0)	(0)
<i>m</i> -DNB	0.59	+1.8	-1.34	+6.7
<i>p</i> -NT	1.32	0	-0.61	+3.1
<i>o</i> -NT	3.03	-1.2	1.10	-5.5
2,4-DNT	1.91 <sup>c</sup>	-0.8 <sup>d</sup>	-0.02	+0.1

<sup>a</sup> These values are taken from the RRKM fitting of the measured rate constants, and differ slightly from the "raw" data plotted in Figure 4. <sup>b</sup> (Δ log *k*)(2.3RT)<sub>1100</sub>. <sup>c</sup> Predicted log *k*(1100; 2,4-DNT) = 1.97 + 1.10 - 1.34 = 1.69. <sup>d</sup> Predicted ΔBDE(2,4-DNT) = 1.8 - 1.2 = +0.6.

result of an intramolecular process 3. This does not imply that under no conditions can phenol formation result from phenyl-NO<sub>2</sub> recombination; these results only show that it does not result under LPHP conditions, where the ratios of scavenger to phenyl radicals and scavenger radicals to phenyl radicals are so large that NO<sub>2</sub> is consumed either by abstracting hydrogen from the scavenger or by oxidizing the scavenger radicals, but not by oxidizing the phenyl radicals (reactions -1' and 4).

The high-pressure rate parameters associated with reaction 1 are shown in Table III. From these parameters the bond dissociation energies for Ar-NO<sub>2</sub> and the Arrhenius parameters for the recombination reaction at 1100 K have been calculated, assuming an unhindered Gorin model<sup>12</sup> for the transition state (see above), and are also shown in that table. The BDE we have obtained for nitrobenzene (71.4 kcal/mol) is in very good agreement with the value of 71.3 kcal/mol selected by McMillen and Golden.<sup>26</sup> From the BDE values for the removal of the NO<sub>2</sub> from *p*-nitrotoluene and 2,4-dinitrotoluene and their heats of formation,<sup>14</sup> the heats of formation of CH<sub>3</sub>-Ph and CH<sub>3</sub>-Ph-NO<sub>2</sub> are determined to be 70.9 and 71.1 kcal/mol, using the thermodynamic relationship Δ*H*<sub>f</sub><sup>°</sup><sub>298</sub>(Ph) = Δ*H*<sub>f</sub><sup>°</sup><sub>298</sub>(Ph-NO<sub>2</sub>) + BDE-(Ph-NO<sub>2</sub>) - Δ*H*<sub>f</sub><sup>°</sup><sub>298</sub>(NO<sub>2</sub>). The rate parameters associated with the reaction of nitrobenzene forming NO (i.e., nitric oxide) and phenol have been determined as log *k<sub>a</sub>* (s<sup>-1</sup>) = (14.3 ± 1.0) - (65.5 ± 5)/2.3RT.

## Discussion

We have carefully chosen a set of nitroaromatic compounds that allows us to determine the effect of methyl and NO<sub>2</sub> substitution on their kinetic behavior. As described above, in all cases the principal initial step is Ar-NO<sub>2</sub> bond scission. The effects of the various substitution on the rate of this step are compared in Table IV. These effects are clearly quite self-consistent and appear to be additive. This can be seen by summing the observed log *k* values for the NB and *m*-DNB, and NB and *o*-NT, to predict the log *k* value for the ArNO<sub>2</sub> which has both a *m*-NO<sub>2</sub> and an *o*-methyl substituent. The agreement between the predicted and measured values is essentially exact. Similarly, the rate constants reported here for NB (forming benzene and phenol) are in very good agreement with those recently measured by Tsang in a heated single-pulse shock tube,<sup>13</sup> log *k* (s<sup>-1</sup>) = (15.4 - 66.0)/2.3RT.

For *o*-NT, on the other hand, preliminary results of Tsang are in some disagreement with those presented here. Although the

absolute rates of *o*-NT decomposition are very similar, the yield of toluene in the heated shock tube is apparently substantially less than the 70-75% observed in the LPHP system, and no other products are detected by the GC. Tests by Tsang to determine whether the shortage of gas-phase products reflects a difference in the initial *o*-NT decomposition reaction or a difference in the scavenging of the initially formed radical have not yet provided a conclusive answer, but a good mass balance of the expected products is observed with *p*-NT.

The identification of the toluene we report in 70-75% yield is certain: the retention time is coincident with (i.e., varies 0.005 min from) that of authentic toluene spiked into the product mixture, and the mass spectrum of that GC peak confirms it as toluene. Cyclohexatriene is a possible product, particularly since ESR studies have implicated, in condensed-phase decomposition, formation of a radical with five protons having equivalent coupling to the radical center, such as would be produced by rearrangement of an initial dinitrophenyl radical to a dinitrocyclohexatrienyl radical. In the present work, cyclohexatriene is ruled out by a retention time difference of 0.35 min, even though as an isomer of toluene it is mass spectrometrically similar.

In addition to agreement on absolute rates, there is some "qualitative" agreement between our results for *o*-NT and those of Tsang, in that our 70-75% yield of toluene is poorer than the 90-95% observed for all the other Ar-NO<sub>2</sub> studied here, and we were not able, by varying pyrolysis conditions (e.g., laser beam intensity, scavenger identity, pressure, etc.), to raise the yield beyond ~75% of the *o*-NT decomposed. On the other hand, with *p*-NT and 2,4-DNT, which has the same *o*-methyl relationship with one of its NO<sub>2</sub> groups, our mass balance was 90% or better, and there was not even a hint of a tendency to undergo a reaction other than Ar-NO<sub>2</sub> scission (or ArOH formation).

In light of this puzzling behavior of *o*-NT, it may be useful to examine the observed effects of methyl and NO<sub>2</sub> substitution on the Ar-NO<sub>2</sub> homolysis kinetics. The BDE values in Table I, as discussed above, are based upon the measured values for the temperature dependence, taken at face value. The stated error limits are random error limits (one standard deviation), determined largely by the scatter in the comparative rate plots. The data provide no firm basis for choosing either activation energies or absolute rates as the preferred indicator of relative BDE values. Given random error limits and the well-known susceptibility of Arrhenius plots to unforeseen systematic errors, the significant point is that the measured absolute rates reflect substituent effects that are additive and thus would seem to constitute a set of very self-consistent data. That is, the effect on decomposition rate of a *m*-NO<sub>2</sub> substituent is the same on going from NB to *m*-DNB as it is in going from *o*-NT to 2,4-DNT (Table IV). Beyond the self-consistency in absolute rates, there are certain trends in the data that suggest the least-squares intercepts and slopes correctly indicate, in most cases, whether the measured rate constants differences are due to activation energy or *A* factor differences.

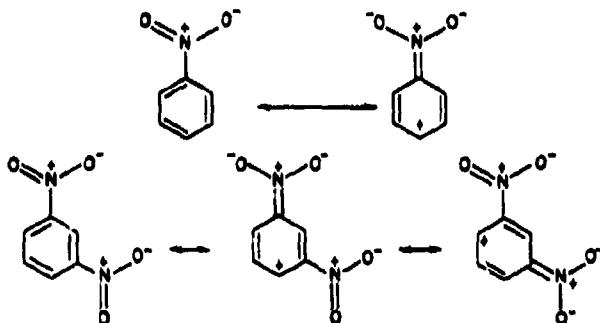
Examination of the rate parameters we have obtained for the nitroaromatics (Tables III and IV) suggests that the changes in the rate constants reflect mainly *A* factor changes. Thus the high value for *o*-NT presumably arises from the greater decreases in the barrier to internal rotation of the methyl and NO<sub>2</sub> groups and from some relief of angle strain as the NO<sub>2</sub> departs, as compared with the reaction of nitrobenzene itself or with *p*-NT. The lower rates for *m*-DNB and 2,4-DNT are associated with slightly higher BDE values (and activation energies) and substantially lower *A*

(14) Lenchitz, C.; Velicky, R. W.; Sikvestro, G.; Schlossberg, L. P. *J. Chem. Thermodyn.* 1971, 3, 689.

(15) Tsang, W., private communication.



factors. Although a slightly tighter transition state (lower  $A$  factor) would be expected with a stronger bond, the large apparent drop in the  $A$  factors cannot be rationalized on that basis alone. An observed  $\Delta \log A = 1.0$  in going from NO to *m*-DNO could be easily ascribed to random errors in the Arrhenius parameters, were it not for the fact that this  $A$  factor drop is almost exactly duplicated in going from *o*-NT to 2,4-DNT. A possible rationalization lies in the fact that a second NO<sub>2</sub> meta to the first decreases the importance of C-N double-bonded resonance structures involving any one of the NO<sub>2</sub> groups.



This "inhibition" will decrease as one of the -NO<sub>2</sub> groups departs, allowing more contribution of a C-N double-bond structure for the remaining -NO<sub>2</sub> group. This will result in an increase in the barrier to internal rotation and a consequent decrease in the  $A$  factor because of the lower rotational entropy of the transition state. (It should be noted that the lower bond-scission  $A$  factors in Table III, have been taken to imply lower overall entropy increases for dissociation. This results in a "compensation" such that all recombination  $A$  factors are similar (i.e.,  $10^{8.3} \pm 0.2$ .)

In the case of *p*-NT, the decrease in rate of decomposition (as compared to NB) is suggested by the Arrhenius parameters to be due entirely to a lower  $A$  factor. In contrast, we would have expected similar  $A$  factors for *p*-NT and NB (since the methyl in the para position should have little impact on relief of strain), and we would have expected the decrease in rate with *p*-methyl substitution to result from a slight strengthening of the Ar-NO<sub>2</sub> bond, rationalizable in terms of inductive stabilization of contributing structures that contain a C-N double bond. In fact, however, the activation-energy-based BDE for *p*-NT is the same as for *o*-NT (though a BDE difference sufficient to cause the observed rate differences would be, at  $\sim 3.3$  kcal/mol, easily within combined standard deviations for the two activation energies) and the rate difference is reflected in a lower  $A$  factor.

The important point is that the rate difference between *p*-NT and *o*-NT (where in the absence of steric effects we would expect little electronic effect) amounts to a difference in free energy of activation of 9 kcal/mol. Thus, even though our results demonstrate that phenyl-NO<sub>2</sub> bonds scission remains the principal

rate-limiting step when an *o*-methyl group is present, the methyl group clearly gives a substantial "push" to the departing NO<sub>2</sub> group. This would seem to be a situation in which some outside influence (e.g., contact with solid surfaces or condensed phases) could trigger some reaction in which one of the hydrogens of the methyl group "pushes" all the way into the nitro group, ultimately transferring a hydrogen to the nitrogen. In other words, the present results indicating Ph-NO<sub>2</sub> bond scission substantially accelerated by an *o*-methyl group show that the strong methyl-NO<sub>2</sub> interaction has not, for an isolated Ar-NO<sub>2</sub> molecule, yet reached the threshold for some different reaction. However, it may be that the extent of "outside" interferences necessary to bring about such a change in *o*-nitrotoluenes is not very great. The nearness of this threshold could be responsible both for the missing products in the shock tube decomposition<sup>15</sup> and for the anomalous behavior of nitrotoluenes reported in the literature.<sup>2,4,6,7</sup> The present results, however, demonstrate that these anomalous effects account, at most, for 25% of the decomposition of nitrotoluene isolated gas-phase molecules at temperatures in the range of 900-1000 °C, and that additional factors must be brought into play in order to open up a new reaction channel that can compete with homolysis of the Ar-NO<sub>2</sub> bond. Having made this determination for mono- and dinitrotoluenes, the question of whether the decomposition of isolated trinitrotoluene molecules also proceeds by C-NO<sub>2</sub> bond scission is now being addressed in our laboratory. Once the behavior of isolated gas-phase molecules is characterized also for trinitrotoluene, then the question of intermolecular interactions that bear on the functioning and malfunctioning of these and similar energetic materials can be addressed.

The effects of methyl and NO<sub>2</sub> substitution on phenyl-NO<sub>2</sub> bond cleavage (Table IV) can be summarized in terms of the effect on the activation-energy-based BDE values on the free energy of activation. The latter approximates the change in BDE if all  $A$  factors were assumed to be equal: (a) *m*-NO<sub>2</sub> substitution increases the phenyl-NO<sub>2</sub> BDE by 2 kcal/mol and  $\Delta G^\ddagger$  by 6.7 kcal/mol; (b) *p*-Me substitution (where there is no steric effect) does not show any effect on the activation-energy-based phenyl-NO<sub>2</sub> BDE, but slows the bond scission rate by a factor of 5 (and therefore raises  $\Delta G^\ddagger$  by 3.1 kcal/mol); (c) for *o*-Me substitution, any electronic effect is overwhelmed by a steric effect, resulting in a net decrease in BDE of 1 kcal/mol and a substantially higher  $A$  factor; (d) when the molecule has both *m*-NO<sub>2</sub> and *o*-Me substitution, the bond-strengthening and bond-weakening effects roughly cancel.

**Acknowledgment.** We acknowledge the support of this work by the U.S. Army Research Office, Contract No. DAAG29-82-K-0169. We appreciate helpful discussions with W. Tsang and the communication of his results prior to publication.

**Registry No.** NB, 98-95-3; *m*-DNB, 99-65-0; *p*-NT, 99-99-0; *o*-NT, 88-72-2; 2,4-DNT, 121-14-2; 1,3-DNT, 99-65-0; NO<sub>2</sub>, 10102-44-0.

Appendix B

LASER-PYROLYSIS OF ETHYLBENZENE:  
THE ROLE OF C-H BOND HOMOLYSIS AT HIGH TEMPERATURES

by

A. C. Gonzalez, C. W. Larson,  
D. F. McMillen, and D. M. Golden

Anales de la Asociacion Quimica Argentina  
73(2) 141-150 (1985)

**LASER-PYROLYSIS OF ETHYLBENZENE: THE ROLE  
OF C-H BOND HOMOLYSIS AT HIGH TEMPERATURES**

**A. C. Gonzalez,<sup>\*†</sup> C. W. Larson,  
D. F. McMillen, and D. M. Golden**

**Department of Chemical Kinetics  
Chemical Physics Laboratory  
SRI International, Menlo Park, CA 94025**

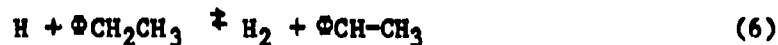
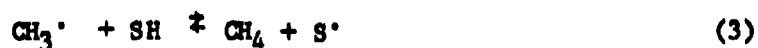
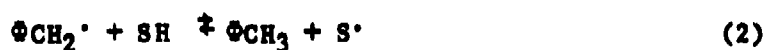
**Submitted to  
ANALES DE LA ASOCIACION QUIMICA ARGENTINA  
Issue dedicated to  
Professor Hans Schumacher  
In Honor of His 80th Birthday**

<sup>\*</sup>Person to whom correspondence should be sent.

<sup>†</sup>Consejo Nacional de Investigaciones Cientificas y Tecnicas de la  
República Argentina.

# ABSTRACT

The mechanism of the thermal decomposition of ethylbenzene has been studied in the temperature range of 1200-1600 K, using laser powered homogeneous pyrolysis. GC/MS analysis shows the final products to consist of toluene, benzene and small amounts of styrene. These products require the conclusion that the rate determining step is the homolysis of the weakest C-C bond in the molecule, producing methyl and benzyl radical, even at temperatures above 1200 K where recent shock tube results<sup>1</sup> had been used to claim initial C-H bond homolysis. The initial homolysis is followed by the reactions with the radical scavenger, and the only styrene formed is that which results from rapid H-atoms chain that result in turn from incomplete scavenging of the methyl and benzyl radicals:



## INTRODUCTION

There are several studies that have reported the mechanism and the Arrhenius parameters for the thermal decomposition of ethylbenzene between 850 and 1100 K. Among these, Leigh and Szwarc,<sup>1</sup> Clark and Price,<sup>2</sup> and Crowne et al.<sup>3</sup> used toluene carrier methods, Kerr and coworkers<sup>4</sup> used an aniline carrier technique, and Robaugh and Stein<sup>5</sup> used the very low-pressure pyrolysis technique. Despite small differences in the rate parameters, there is general agreement that the reaction mechanism involves, as the first step the breaking of the C-C bond (the most thermodynamically favored bond homolysis in the molecule) to form benzyl and methyl radicals.



Recently Brouwer, Muller-Markgraf and Troe<sup>6</sup> have reported ethylbenzene decomposition in the temperature range of 1250-1600 K in a shock tube. Based on the observation of the UV spectra of the primary products as well as on the formation of styrene as the only final product, they conclude that the primary decomposition step must be a C-H bond split in the ethyl

group with high-pressure Arrhenius parameters of  $10^{17.1} \text{ s}^{-1}$  and 81.3 kcal/mol.



Since C-H bond homolyses in general are not competitive with C-C bond homolyses at more moderate temperatures, the rate parameters of any of the former class of reactions, with one recent exception,<sup>7</sup> have not been characterized. Consequently, Brouwer and coworkers have taken the high-temperature formation of styrene as indicating that C-H bond scission reactions have very high A-factors along with their high activation energies, such that they become important at very high temperatures, even though they are unimportant at lower temperatures. Because of the general implications of this conclusion for high-temperature reactions of hydrocarbons, it is important to test its validity by independent measurements.

The apparently contradictory results cited above cannot be reconciled easily by invoking crossover at the higher temperature of the shock tube to a higher A factor, higher activation energy process. That is, even if the reaction has two accessible channels, a complete change in the reaction mechanism so that at temperatures below 1200 K, toluene is the major product, and at higher temperature, styrene is the only product, would not be expected. Consistent with this expectation, Tsang has recently determined the products of ethylbenzene decomposition up to 1300 K in a shock tube and found styrene as only a minor product.<sup>8</sup> In order to fully resolve remaining uncertainties about competing pathways we have studied the reaction by a technique which makes accessible the full 1200 to 1600 K temperature range used in the shock tube work of Brouwer et al.<sup>6</sup>

## EXPERIMENTAL

The technique used in this work, laser-powered-homogeneous-pyrolysis (LPHP), is a modification of the technique first described by Shaub and Bauer<sup>9</sup> in which an infrared laser is used to heat an absorbing but unreactive gas, which then collisionally transfers its energy to the substrate. The modification of the method used<sup>10</sup> here incorporates a heated flow system and a pulsed infrared laser (Lumonics K-103). The heated flow system makes the technique suitable for study of substrates with very low room temperature vapor pressure. The use of a laser, which is repeatedly pulsed for very short periods, and the rapid expansion wave-cooling, which takes place after each pulse, helps to minimize secondary reactions. Scheme 1 shows the LPHP flow system.<sup>10</sup> A slow flow of SF<sub>6</sub> (infrared absorber), CO<sub>2</sub> (inert collider), cyclohexane (temperature standard), cyclopentane (radical scavenger) and substrate were passed through the reactor, a gas chromatographic sampling valve, a needle valve and into a vacuum pump. The reactor and the flow line were heated to 313 K to avoid condensation problems. Flow was maintained at the desired level by adjusting the first needle valve, and total pressure was maintained at 110 Torr by adjusting the second needle valve. A small portion of the cell was irradiated with the P20 line = 10.6  $\mu\text{m}$  of a Lumonics K-103 CO<sub>2</sub> laser (duration 1  $\mu\text{s}$ ) at a constant repetition rate (0.25 Hz) until a new steady state of product and undecomposed substrate was attained (Scheme 2). The cell had KCl window to transmit the IR radiation, a 1.2 cm<sup>2</sup> laser aperture to define the heated volume and a rear reflecting mirror to maintain axial

temperature homogeneity while absorbing approximately 20% of the incident laser radiation in a single pass. The reaction temperature was controlled by decreasing the IR radiation energy and the SF<sub>6</sub> content of the gas mixture. The flow time and irradiation frequency provided at least 20 laser shots during the average lifetime of a substrate molecule in the cell and assured complete gas mixing between shots. In all the experiments the products have been identified by using a GC equipped with a mass selective detector (Hewlett-Packard models 5880 A and 5970 A) and the average concentration of reactant and products were measured gas chromatographically using a FID detector.

Measurement of the temperature corresponding to any particular measurement of *k* or % decomposition of the ethylbenzene is accomplished by the concurrent determination of the fractional decomposition of a temperature standard. Cyclohexene was chosen as a temperature standard to measure the temperature dependence of the ethylbenzene decomposition because of its well known kinetic parameters, the stable products it forms and because its activation energy is close to the activation energy of the substrate.<sup>9</sup>

Under "steady-state," laser on conditions the decrease in average concentration of a substrate A during any single laser shot equals the replenishment (by flow) of A before the next laser shot. This leads to equation

$$k\tau_r = -\ln \left[ 1 - \left( \frac{[A]_0}{[A]_{ss}} - 1 \right) \frac{V_T}{V_R} \left( \frac{\tau_l}{\tau_f} \right) \right]$$

where *k* is the first order rate constant describing disappearance of A,  $\tau_r$  is the reaction time (10  $\mu$ s) following each laser pulse,  $\tau_l$  is the time between laser pulse (4 s),  $\tau_f$  is the flow lifetime in the reaction cell (typically 200 s),

$V_T$  and  $V_R$  are the total and laser heated cell volumes and  $A_0$  and  $A_{ss}$  are the laser-off and laser-on steady state concentration, respectively.



The degree of falloff for cyclohexene was estimated using RRKM calculations based on a vibrational transition state and a collision efficiency of  $\beta = 0.1$ . This resulted in Arrhenius parameters under the LPHP conditions of  $\log k_{uni} (\text{sec}^{-1}) = 14.3 - 61.9/\theta RT$  (versus  $\log k_{\infty} (\text{sec}^{-1}) = 15.15 - 66.6/\theta RT$ ).

## RESULTS AND DISCUSSION

The final products of the pyrolysis of ethylbenzene, without an added radical scavenger and under LPHP conditions that provided up to 70 % decomposition of the substrate, are toluene, benzene, ethylene, styrene, and methane (Figure 1). In order to suppress the chain decomposition and determine whether styrene formation results from the following reactions:



or from another set of reactions (i.e., the C-H homolysis invoked by Brouwer et al.), we ran a series of experiments with different amounts of cyclopentane added as inhibitors. Under these conditions, styrene and the low molecular-weight hydrocarbons formed by degradation of the aromatic ring decreased substantially compared with the above experiments, and toluene and benzene increased to 90-95% of the final aromatic products (Figures 2 and 3). The product distributions resulting from the decomposition of ethylbenzene in the

presence of varying amounts of radical scavenger at different temperatures are summarized in Table 1.

Although styrene appeared as a final product only in very small amounts at different temperatures when a scavenger was present, the question of its thermal stability and its possible reactions under the experimental conditions had to be addressed. Accordingly, styrene decomposition was studied under the same conditions of temperature and scavenger as had been used with ethylbenzene, and the results are presented in Table 2. We are not able at this time, because of the many possible reactions that can take place at this high temperature, to definitively state whether the styrene decomposition results primarily from displacement by hydrogen atoms or by another mechanism. The experiments with styrene were performed merely to provide a rough measure of the extent to which initially formed styrene would be consumed under the experimental conditions of the ethylbenzene pyrolysis. The amounts of styrene shown in Table 1 have been adjusted for this consumption in secondary reactions in order to reflect total styrene production.

Based on the above results, we are forced to conclude that even above 1250 K, the first step of the thermal decomposition of ethylbenzene is the breaking of the weakest C-C bond, to give benzyl- and methyl- radicals (reaction 1). This is followed by the reactions of these radicals with the scavenger (when it is present) or with the substrate. Since in the presence of a fifty-fold excess of inhibitor, styrene formation is almost

completely suppressed, its formation is entirely consistent with the well known set of reactions 4-6:



Thus our results, in agreement with those of Rossi and coworkers,<sup>7</sup> do not justify the invoking of unusually high A-factors for C-H bond scission. We find this reassuring in that the obvious transition-state picture is that the entropy of activation for C-H scission cannot easily be more positive than for scission of larger fragments.

The presence of benzene can be attributed to several reactions in the framework of the complex chemistry which occur during ethylbenzene decomposition at such high temperatures. It is most probably formed as a result of the H atom induced decomposition of toluene or ethylbenzene, and in fact provides another indicator (in addition to styrene formation) that radical scavenging is not complete.

We emphasize it was not our purpose to determine precisely the rate parameters of the ethylbenzene pyrolysis, but to determine the product yields under well defined condition between 1200 to 1600 K. This means that we carried out the experiments under conditions of very high fractional decomposition that are not suited for accurate determination of the rate constant or the effective reaction temperature. However, from our results we are able to make some comments about the relative rate constants

for a C-H and C-C bond homolysis. In fact, the data set an upper limit to the ratio of C-H to C-C bond breaking ( $k_1/k_1$ ). If we assume that all styrene comes from the C-H bond homolysis, and that at the highest levels of scavenger, the H atom produced in reaction<sup>5</sup> were prevented from propagating a chain, then the rate ratio would be given by the styrene/toluene ratio. This value of  $k_1/k_1$  ( $\sim 0.06$  at 1470 K) is an upper limit in that the chain length might be greater than 1, and in that the pool of allyl radicals in equilibrium with diallyl will be significant at temperatures in the 1500 K range. The latter factor will unavoidably result in the production of a significant amount of styrene via reactions (8) and (5). In fact, an estimate, based on equilibrium data in the literature,<sup>11</sup> of



the allyl radical concentration in equilibrium with the diallyl accumulated at 50% ethylbenzene decomposition accounts for a significant part of the observed styrene production. This illustrates the fact that effective radical scavenging becomes inherently more difficult with increasing temperature. Since the scavenger operates by converting a more reactive radical to a less reactive radical  $S^\cdot$  (that is, a radical that forms weaker bonds to hydrogen and carbon), and since the termination reaction then becomes dimerization of the scavenger radicals, it is unavoidable that the weaker as an abstractor that a scavenger radical  $S^\cdot$  is, the higher will be the concentration of  $S^\cdot$  in equilibrium with the termination product  $S_2$ . The above estimate of styrene production initiated by scavenger radicals, if taken at face value, allows us to decrease the upper limit of the C-H to C-C bond scission ratio to 0.03.

This conclusion is amplified and indicated to be conservative if we use RRKM theory to calculate the rate constants for the two channel thermal decomposition of ethylbenzene. When we use the known heats of formation for the radicals and corresponding reductions in vibrational frequencies for the complex in each of the two transition states, we obtain a value close to the known rate constant for the C-C bond homolysis path but a very much smaller rate constant for the C-H bond breaking (more than  $10^{1.5}$ ). In order to reproduce Brouwer's results we had to assume not only a very much looser transition state for the C-H channel, but also had to reduce by 10 kcal the reported heat of formation of the  $\Phi\text{CH}-\text{CH}_3$ . For the C-C channel, we had to assume a very tight transition state and we had to increase by 10 kcal the known heat of formation of the radical formed in that reaction ( $\Phi\text{CH}_2$ ). In other words, to reproduce Brouwer's reported observation of styrene as the sole product, we had to assume wholly inconsistent transition state models for two rather similar bond scission processes. This involves a much looser transition state for C-H bond scission than for C-C bond scission, and relative BDE values 20 kcal/mol different than the accepted literature values.<sup>11</sup> The unreasonableness of these requirements is entirely consistent with our experimental observation that no styrene is produced by C-H bond homolysis.

#### Acknowledgement

The authors gratefully acknowledge the support of this research by the U.S. Army Research Office, under Contract No. DAAG29-82-K-0169.

#### REFERENCES

1. C. H. Leigh and M. Szwarc, J. Chem. Phys., 20 844 (1952).
2. W. D. Clark and S. J. Price, Can. J. Chem., 48, 1059 (1970).
3. C.W.P. Crowne, V. J. Grigulis, and J. J. Throssell, Trans Faraday Soc., 65, 1051 (1969).
4. J. A. Kerr, A. F. Trotman-Dickenson, and M. Wolter, J. Chem. Soc., 3584 (1964).
5. D. A. Robaugh and S. E. Stein, Int. J. Chem. Kinetics, 13, 445 (1982).
6. L. Brouwer, W. Müller-Markgraf, and J. Troe, Ber Bunsenges. Phys. Chem., 87, 1031 (1983).
7. M. Rossi, D. F. McMillen, and D. M. Golden, J. Chem. Phys., in press.
8. W. Tsang, private communication.
9. W. M. Shaub and S. H. Bauer, Int. J. Chem. Kinetics, 7, 509 (1975).
10. D. F. McMillen, K. E. Lewis, G. P. Smith, and D. M. Golden, J. Phys. Chem., 86, 709 (1982).
11. M. Rossi, K. D. King, and D. M. Golden, J. Amer. Chem. Soc., 101, 1223 (1979).
12. D. F. McMillen and D. M. Golden, Ann. Rev. Phys. Chem., 33, 493 (1982).

Table 1  
PRODUCTS YIELDS IN ETHYLBENZENE PYROLYSIS WITHOUT SCAVENGER<sup>1</sup>

$C_2 + CH_4$ <sup>2</sup>	Benzene	Toluene	Styrene
64.4	9.5	25.7	15.3
91.8	12.9	31.0	12.4
246.3	12.9	17.7	4.6

PRODUCTS YIELD IN THE INHIBITED REACTION\*

$\Phi_{ET/SH} = 1/10$

T	Benzene	Toluene	Styrene
1470	9.4	13.1	2.2
1480	11.6	17.1	2.7
>1500	26.0	34.5	12.8
>1500	19.1	36.9	15.6

$\Phi_{ET/SH} = 1/100$

1250	1.7	5.6		
1370	6.2	10.2	0.8	0.9 <sup>3</sup>
1370	5.9	9.9	0.8	0.9 <sup>3</sup>
1380	6.9	13.9	0.8	0.9 <sup>3</sup>
1470	13.0	22.6	1.2	1.8 <sup>3</sup>
>1500	40.4	25.6	4.4	6.7 <sup>3</sup>
>1500	42.7	19.8	4.1	6.3 <sup>3</sup>
>1500	52.5	22.8	5.3	9.7 <sup>3</sup>

<sup>1</sup>Molar yield expressed as % of ethylbenzene initial.

<sup>2</sup> $\Sigma(C_1 + C_2)$  formed from degradation of the aromatic ring. Note that for 100% decomposition, the sum of yields can be >200% even without ring degradation.

<sup>3</sup>Styrene formation corrected for decomposition in secondary reactions.

Table 2  
PRODUCTS YIELDS IN THE INHIBITED DECOMPOSITION OF STYRENE\*

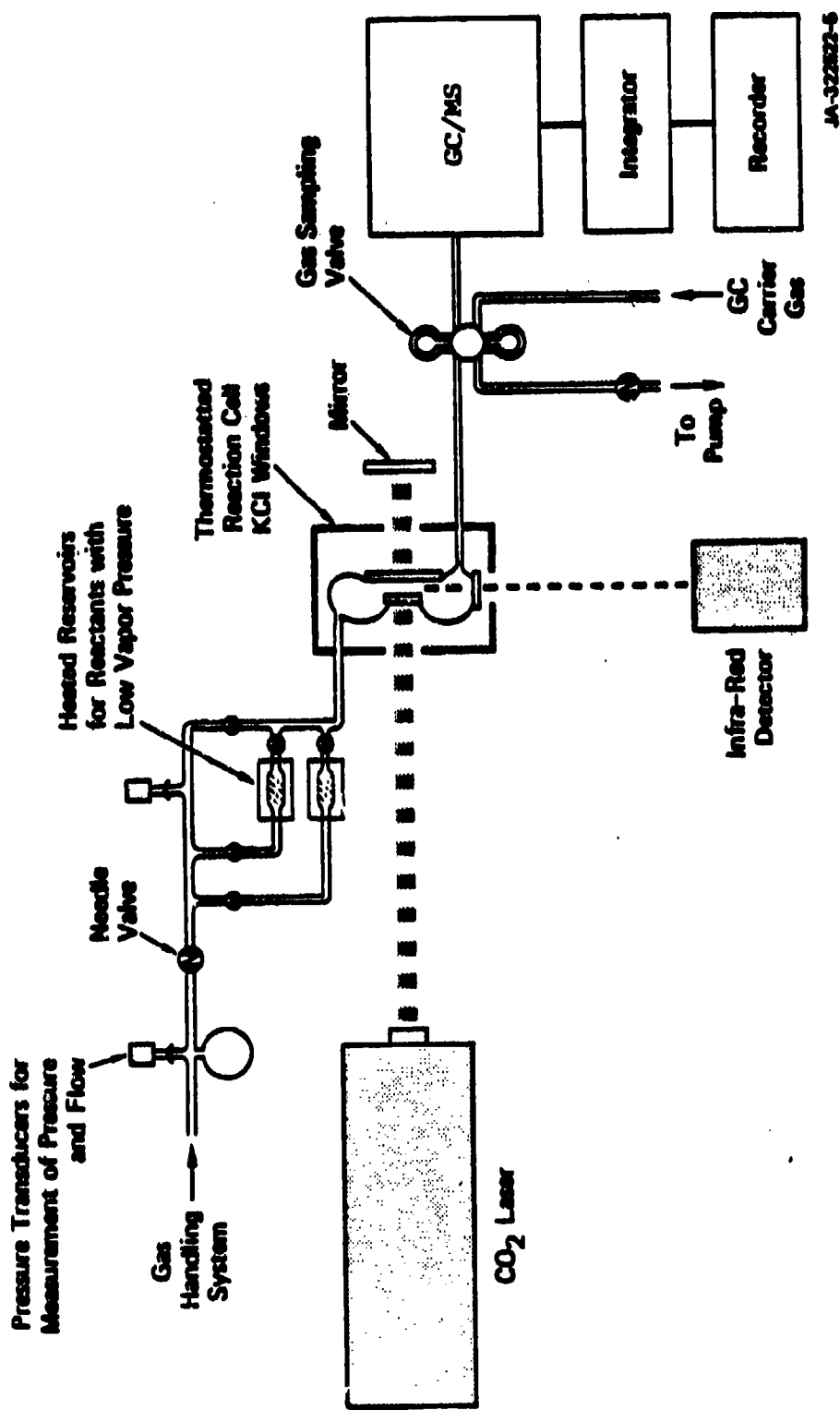
Styrene/SR = 1/100

T	Benzene	Toluene
1320	5.1	0.55
1330	3.4	1.8
1340	7.0	2.1
>1500	46.0	6.5

---

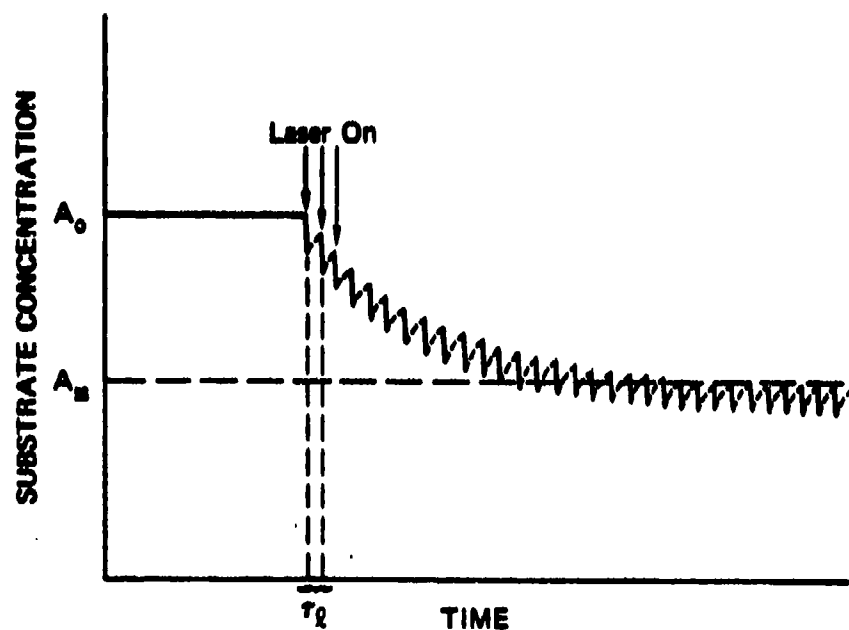
\*Molar yield expressed as % of styrene initial.





JA-32552-5

SCHEME 1 LASER-POWERED HOMOGENEOUS PYROLYSIS FLOW SYSTEM



JA-322822-6

**SCHEME 2 REPRESENTATION OF THE SPATIALLY AVERAGED  
SUBSTRATE CONCENTRATION AS A FUNCTION OF TIME**

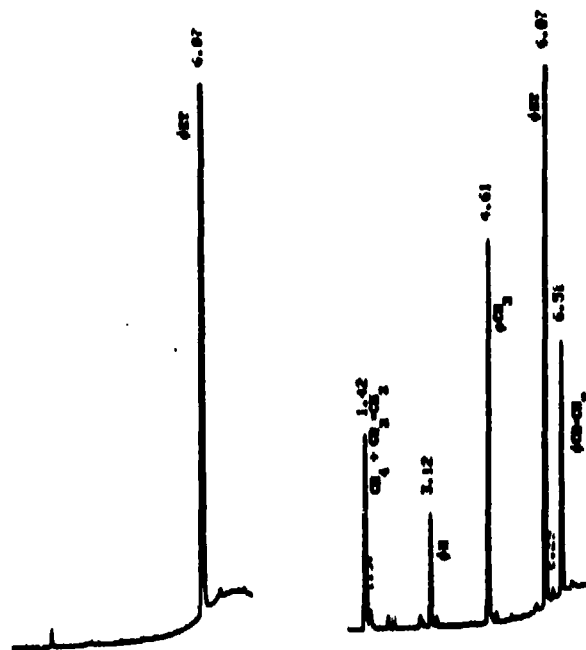


FIGURE 1 GC OF ETHYLBENZENE AND OF THE PRODUCTS OF ETHYLBENZENE DECOMPOSITION WITHOUT SCAVENGER (50% REACTION)

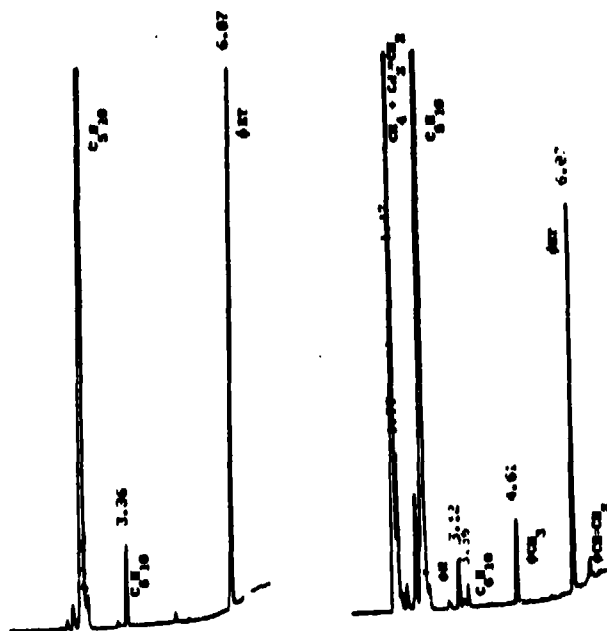


FIGURE 2 GC OF THE PYROLYSIS PRODUCTS OF ETHYLBENZENE, CYCLOPENTANE AND CYCLOHEXENE WITH SCAVENGER/SUBSTRATE = 10/1 AT 1500 K, ILLUSTRATING SUPPRESSION OF STYRENE FORMATION BY SCAVENGER.

